Plan and Current Status of Plasma Wall Interaction Study in KSTAR

May 22, 2007

presented by Si-Woo Yoon

National Fusion Research Center

핵융합연구센터
National Fusion Research Center

Outline

- Introduction
- Operation plan
- 1st Plasma
- Design of PFCs
- Edge modeling activities

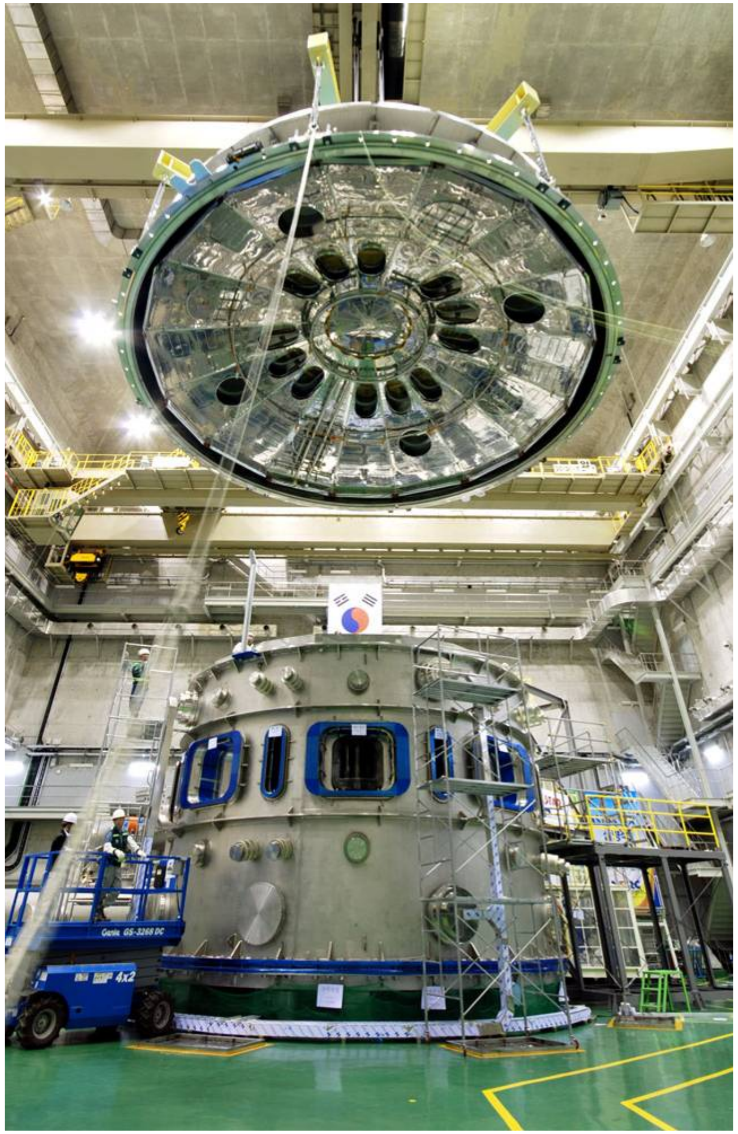

Introduction and operation plan of KSTAR

KSTAR Key parameters

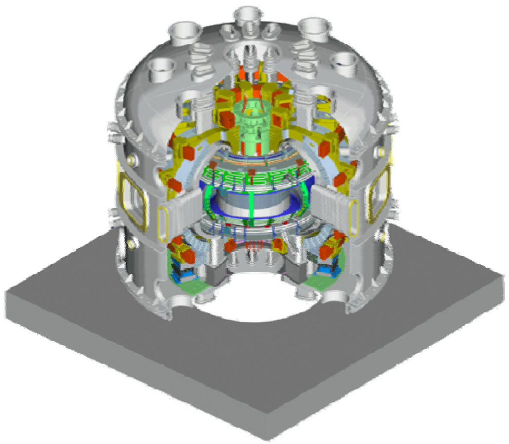

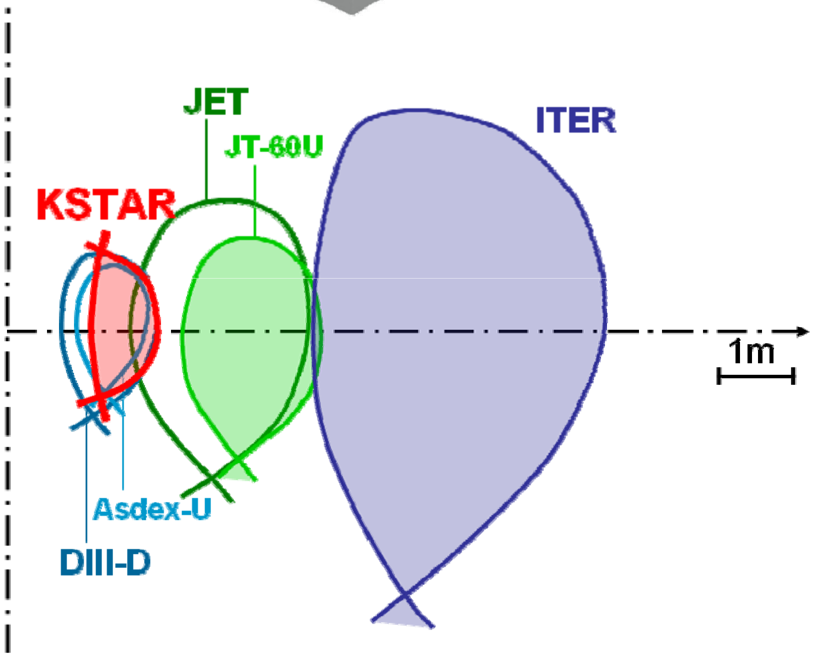

PARAMETERS	KSTAR	ITER
Major Radius, R_0	1.8 m	6.2 m
Minor Radius, a	0.5 m	2.0 m
Plasma Current, I_P	2.0 MA	15 MA
Elongation, κ	2.0	1.7
Triangularity, δ	0.8	0.33
Toroidal Field, B_0	3.5 Tesla	5.3 Tesla
Pulse Length	300 sec	400 sec
Dimension	8.6 m (H)	24 m (H)
	8.8 m (D)	28 m (D)
Superconductor	Nb_3Sn, NbTi	Nb_3Sn, NbTi
Magnet Weight	270 Ton	10,135 Ton
Cryogenic System	9 kW	72 kW

Mission of KSTAR Project

- To develop a steady-state-capable advanced superconducting tokamak
  - Superconducting TF and PF magnet system
  - Non-inductive current drive system
  - Long-pulse diverter and PFC system
  - Real-time plasma profile control system
- To establish the scientific and technological base for an attractive fusion reactor as a future energy source
  - High-performance AT mode research
  - Active control tools of the high beta MHD instabilities
  - Flexible heating & CD system
  - Advanced diagnostics

KSTAR Long-Term Plan

Phase-1 — **Initial Operation H-mode Operation**

↓

Phase-2 — **Steady-State Operation Research** ⟷ ITER Pilot Device

↓

Phase-3 — **High-beta AT-Mode Research** ⟷ ITER Satellite Device

↓

Phase-4 — **Steady-State AT-mode Research** ⟷ DEMO Pilot Device

KSTAR Way to Fusion

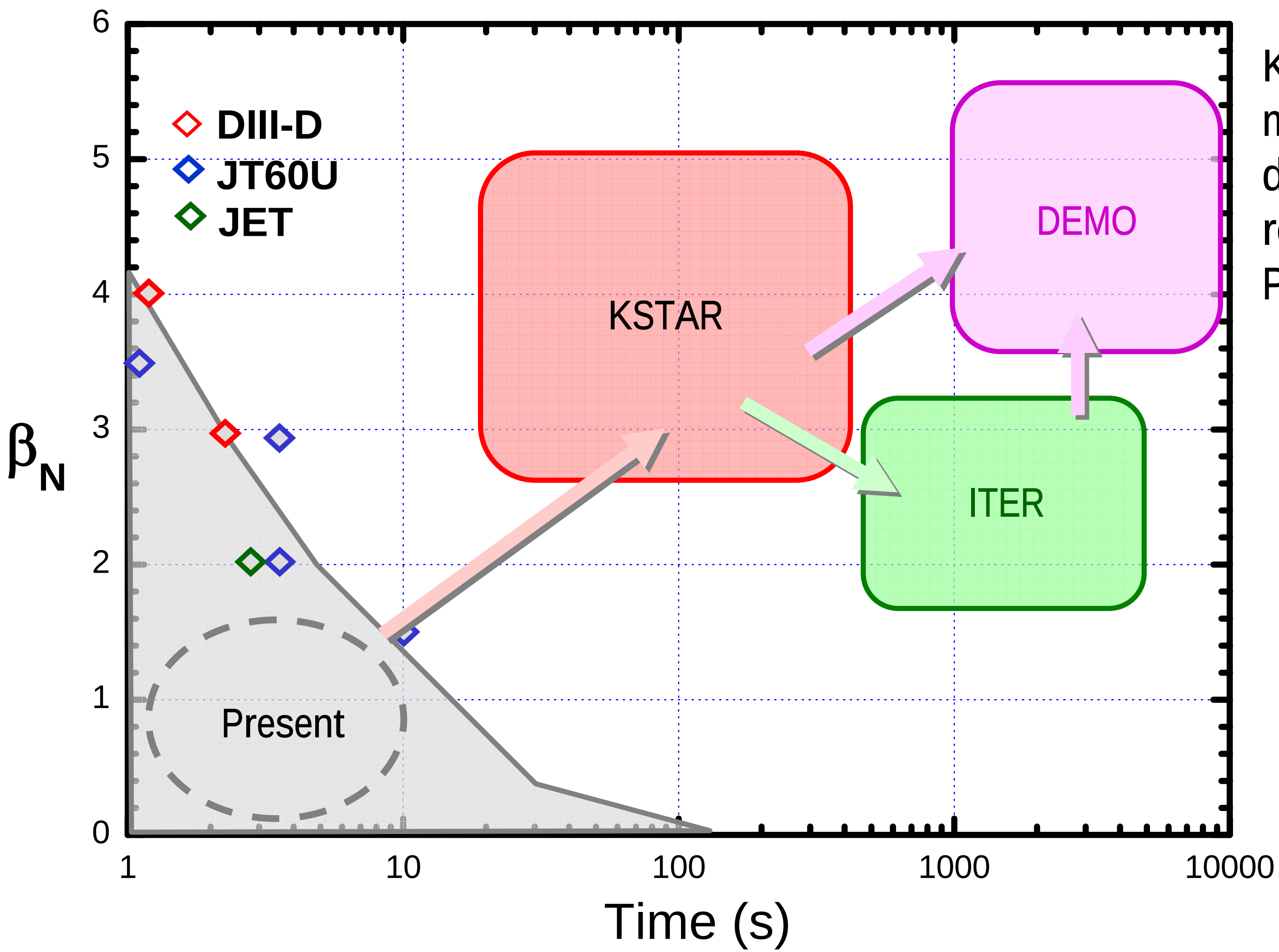

KSTAR is the most efficient device for ITER relevant and Demo Physics Operation.

Superconducting magnet System

- SC Coils
  - Superconductor : Nb_3Sn (TF & CS & PF)
    NbTi (PF 6,7)
  - Cable : Cable-in-conduit conductor
  - Cooling : Supercritical helium (5 K, 6 bar)
- Structures
  - Structure : SS316LN
  - Peak magnetic force : 15 MN

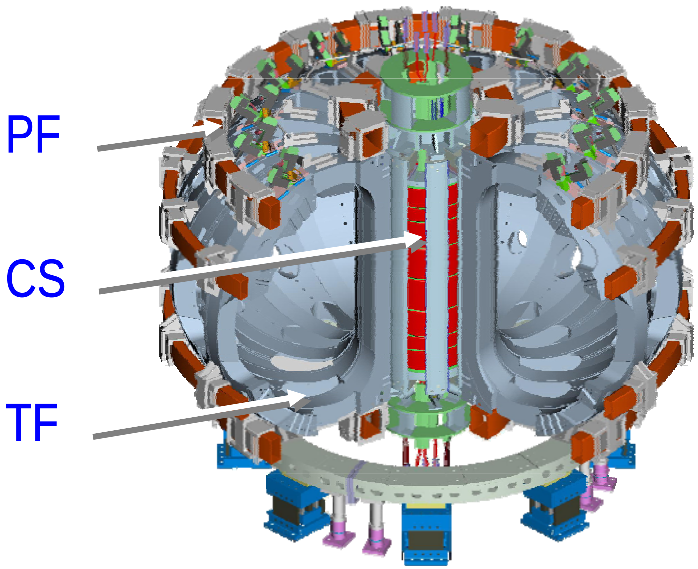

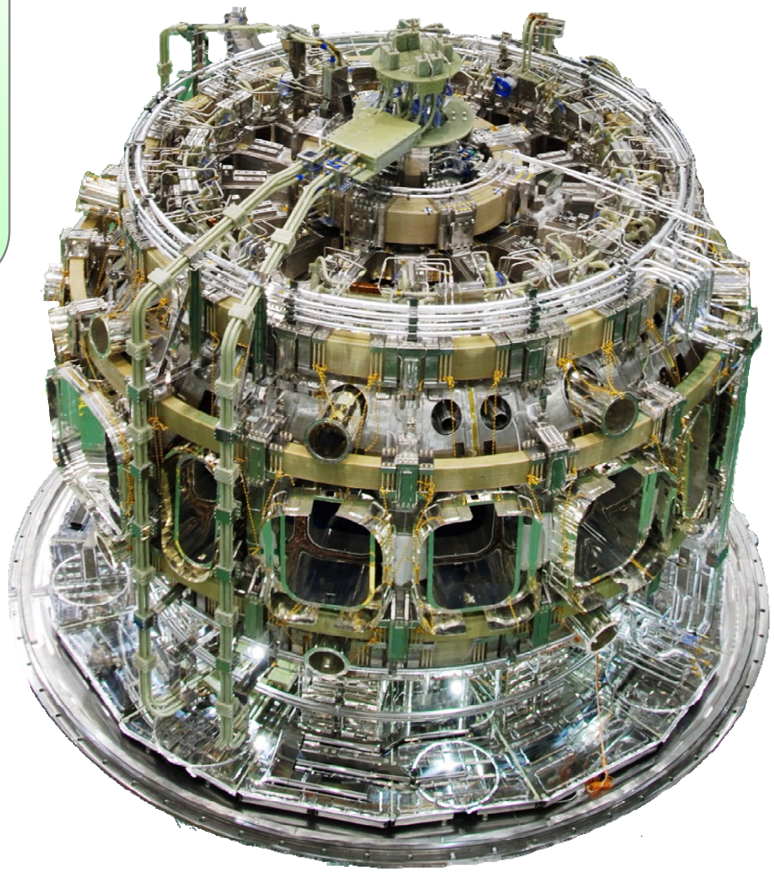

Shaping and Position Control

Strong Plasma Shaping ($\kappa_x \leq 2.0$, $\delta_x \leq 0.8$)

- High-n ideal ballooning stability
- Low-n external kink stability

- Peeling-ballooning stability etc.
- Passive plate close to the plasma
- Slowing down of vertical position instability

Segmented In-vessel Coil

- Simplification in the fabrication, installation, and maintenance

- IVC, IRC, FEC/RWM control coil
- Simultaneous control of the axisymmetric and non-axisymmetric modes

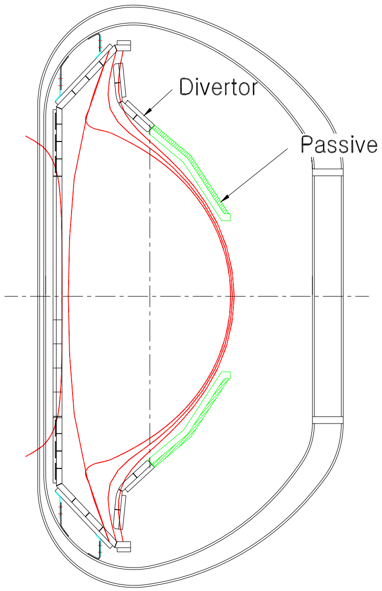

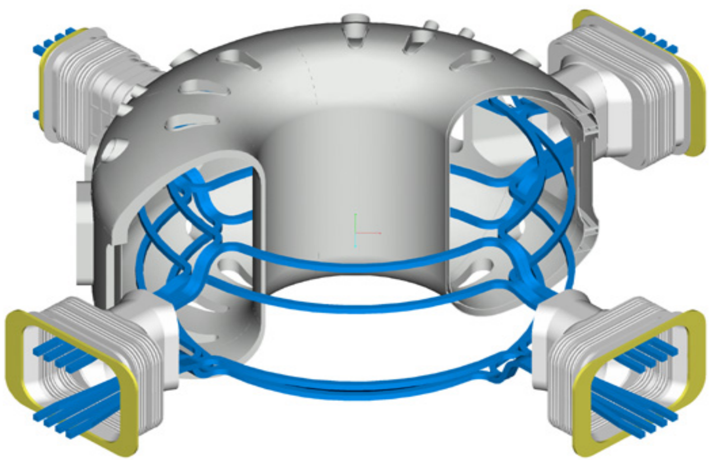

In-Vessel Control Coil System

- In-vessel control system to be installed for the simultaneous control of n=0 position and non-axisymmetric FEC & RWM control
- In n=2 up-down symmetric configuration, ELM suppression using RMP

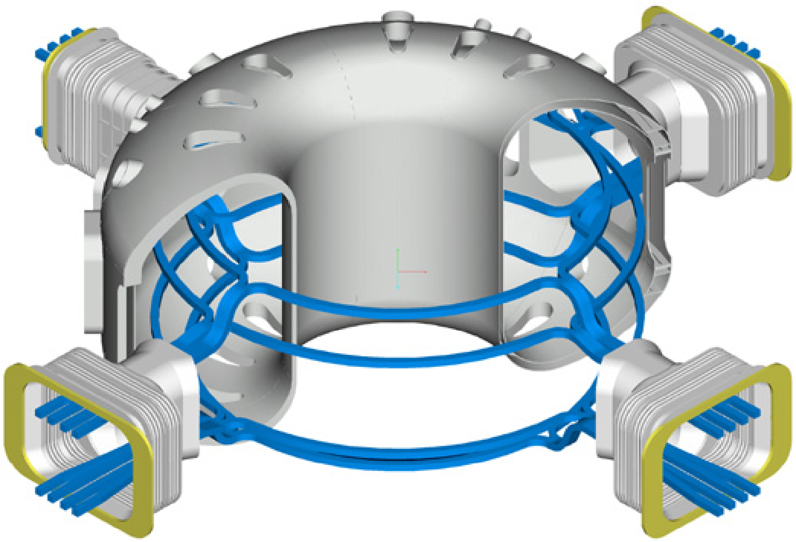

• **Utilizing toroidal segmentation concept for easy fabrication and installation**

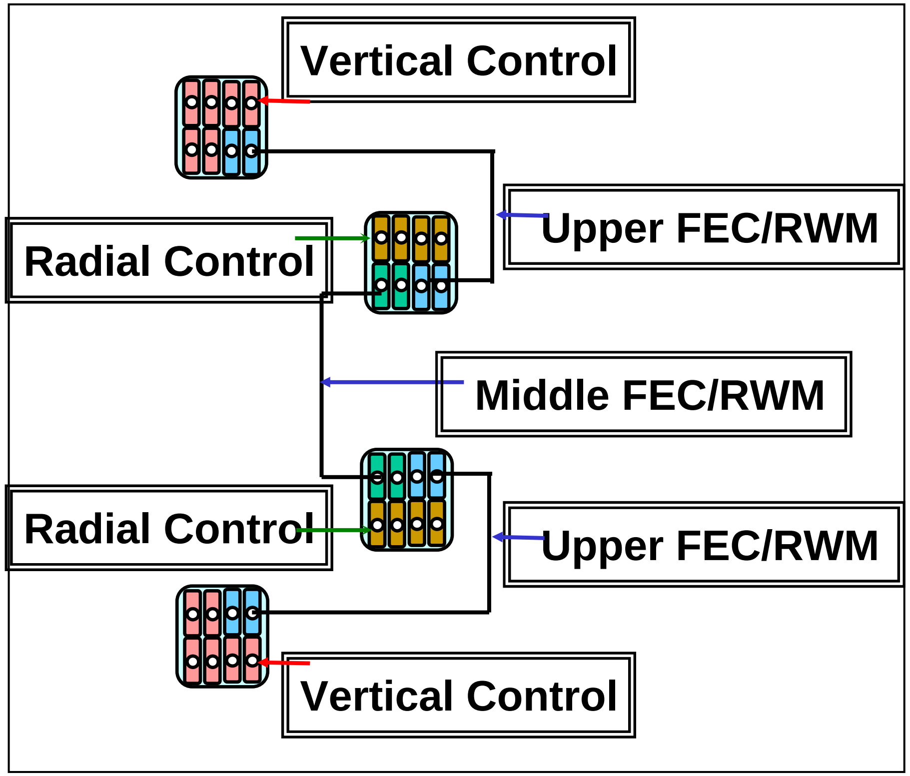

Construction Milestones

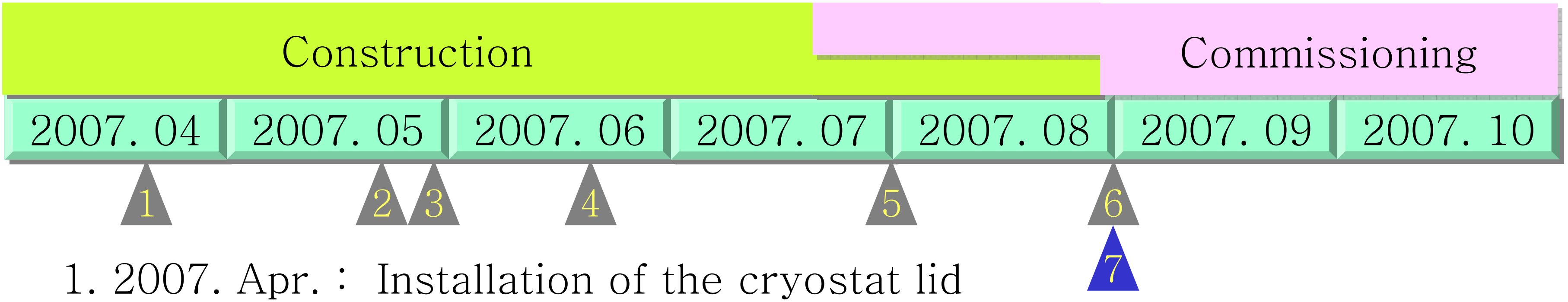

1. 2007. Apr. : Installation of the cryostat lid
2. 2007. May : Start of VV vacuum commissioning
3. 2007. May : Start of cryostat vacuum commissioning
4. 2007. Jun. : End of 1st VV vacuum commissioning
   Installation of ancillary system for 1st plasma
5. 2007. Jul. : End of 2nd VV vacuum commissioning
6. 2007. Aug. : End of cryostat vacuum commissioning
   Machine construction finish
7. 2007. Sep. : Start of integrated commissioning
8. 2008. Jun. : First Plasma

Tokamak & Vacuum Pumping Systems

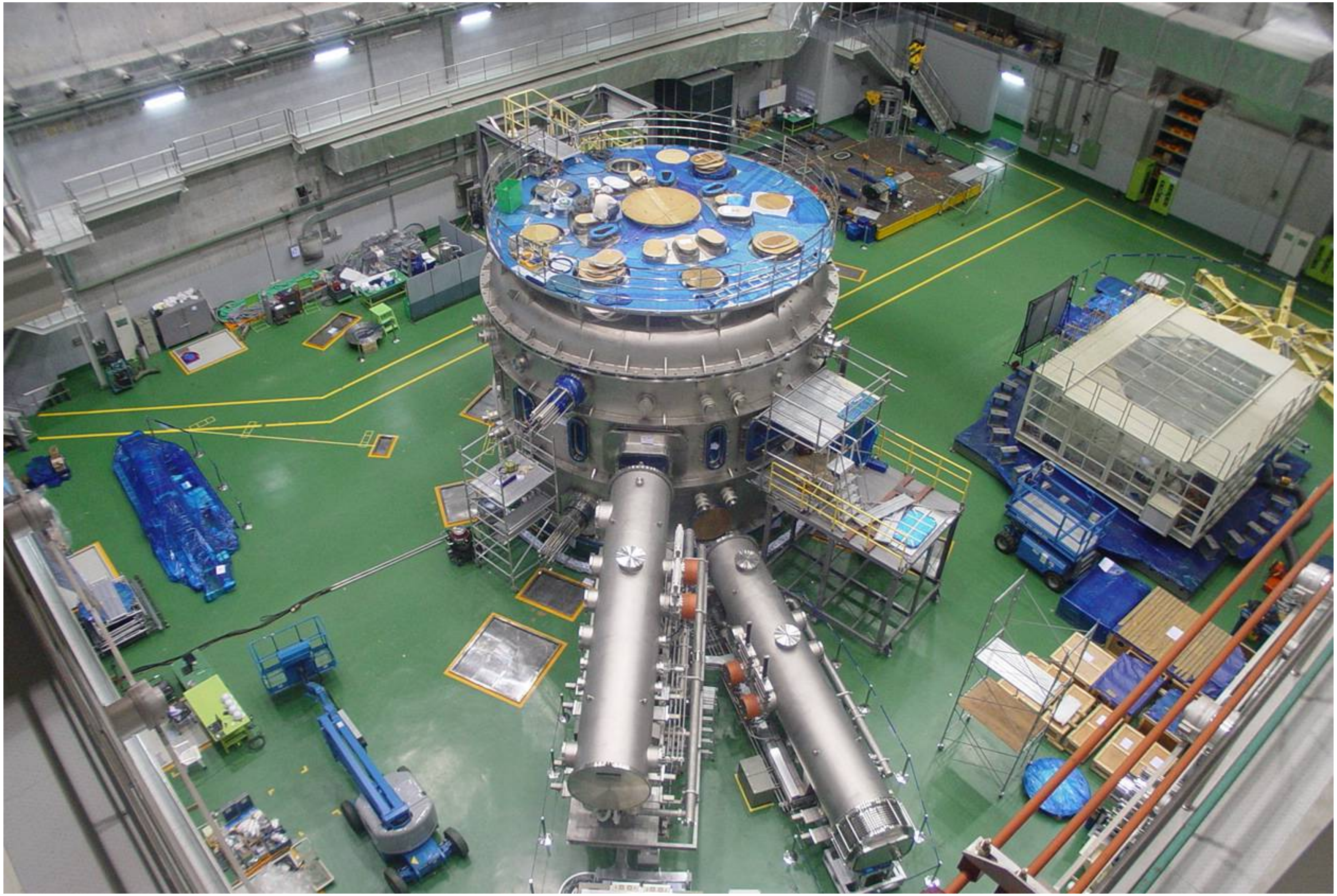

Ancillary System Development Plan

Operation Phase	Initial Operation				Baseline Long-pulse Operation				
Year	2007	2008	2009	2010	2011	2012	2013	2014	2015
Operation Mode		First Plasma	Circular Ohmic	Shaped Ohmic	L- & H-mode	Long-pulse H-mode	Hybrid	Long-pulse Hybrid	RS-mode
NBI (MW)				2.7	5.4	5.4	5.4	5.4	7.4
ICRH (MW)	1.5	1.5	1.5	1.5	1.5	1.5	1.5	3.0	3.0
LHCD (MW)						1.5	1.5	1.5	3.0
ECCD (MW)	(0.5)			1.0	1.0	2.0	2.0	3.0	3.0
Diagnostics	Basic	Base-I	Base-II	Base-III	Base-IV				
In-vessel coil				Position	FEC/RWM				
PFC		Inner-limiter		Divertor, P. P.					
Plasma Control				Position, Shape	FEC	ELM	NTM		RWM
Fueling/ pumping	Gas-puffing			Divertor Pumping	HFS-Pellet				
MPS	50MVA		100MVA		MG: 1.6GJ	SN(PF3-6)			

Initial Operation Plan ('08-'10)

KSTAR

Major Goals

- Commissioning and first-plasma generation
- Development of basic operation skill of superconducting tokamak
- Circular and shaped Ohmic plasma experiments
- Development of ancillary systems for long-pulse operation
- Development of international collaboration framework

(2008.6)	• **First-Plasma Exp.** - pre-ionization test - low dI_p/dt	$I_p \leq 200$ kA ECH 500kW
Campaign-1 (2009)	• **Circular Ohmic Plasma Exp.** - Plasma current ramp-up - RF/plasma interaction & fast ion physics	$I_P \leq 1$ MA ICRH 2 MW
Campaign-2 (2010)	• **Shaped Plasma Exp.** - H-mode exp. - Plasma position & shape control - Heating/CD test (NBI, ICRH, ECH)	Double null shape $I_P \leq 2$ MA NBI 2.7 MW

Baseline Long-Pulse Operation (11'-15')

- **Major Goal**
  - Increase of pulse length (20 ->300 sec) and input power (5 -> 16MW)
  - Test of PS, heating/CD, PFCs, control, diagnostics systems etc.
  - Basic physics study in long-pulse operation condition
  - Real-time control for MHD instabilities (FEC, NTM, ELM etc.)

	2011	2012	2013	2014	2015
Experiment Mode	**L & H-mode**	**Long-pulse H-mode**	**Hybrid Mode**	**Long-pulse Hybrid mode**	**RS-mode**
Pulse-length	**>20**	**>50**	**>50**	**>100**	**>100**
Input-power(MW)	**7.9**	**9.4**	**10.4**	**12.9**	**16.4**
NBI	**5.4**	**5.4**	**5.4**	**5.4**	**7.4**
ICRH	**1.5**	**1.5**	**1.5**	**3.0**	**3.0**
LHCD		**1.5**	**1.5**	**1.5**	**3.0**
ECCD	**1.0**	**1.0**	**2.0**	**3.0**	**3.0**

KSTAR

Year	07–12	13–17	18–22	23–25
Objective	Phase I	Phase II	Phase III	Phase IV
Operation Goal	Initial Operation	Steady-state Operation Research	High beta AT Operation	Steady-state AT
Activities	• First Plasma • SC Tokamak Operation Technology (3.5 T) • D-shaped Plasma (1 MA) • H-mode Operation	• Long Pulse Operation (over 100 s) • AT Operation Technology (< 20 MW) • ITER Pilot Device	• Long Pulse Operation (over 300 s) • AT Operation Stabilization (> 20 MW) • ITER Satellite	• High beta AT mode & long pulse • Material Test for DEMO

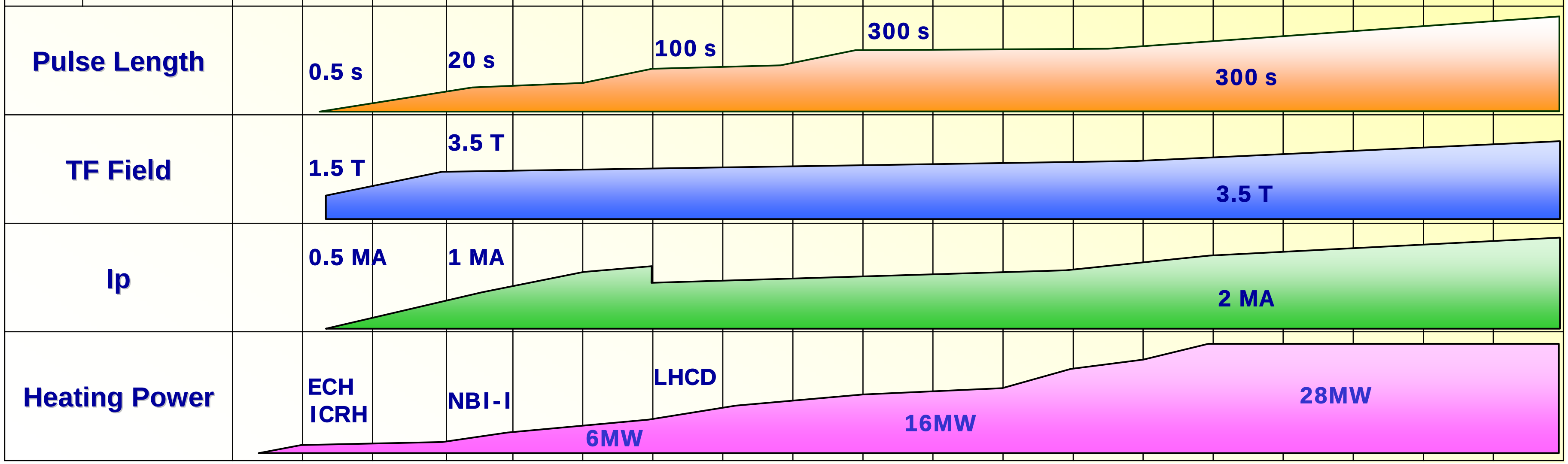

Considerations for 1st plasma

First Plasma

- **Low loop voltage & low magnetic flux startup** (< 0.4 V/m, ~0.7 Wb)
  - *Plasma control system operation (RFM digital control)*
  - *BRIS (Blip resistor insertion system)*
  - *Optimum discharge using SC PF coil & double-walled VV*

- **Pre-ionization startup**
  - ECH(84Ghz, 500kW) fundamental : B_T = 2.4 ~ 3.5 T
    - *well proven technique by many tokamaks*
  - ECH 2nd harmonic : : B_T = 1.3 ~ 1.7 T
    - *recent experiments by JT60U, DIII-D, …*
  - ICRH vacuum eigen-mode pre-ionization
    - *recent experiments by Tore-Supra, Textor, …*
    - *further modeling is on-going*

- **PFC & wall conditioning**
  - Baking(<150C), GDC(boronization), ICR cleaning, ...
  - Inboard limiter & poloidal limiter

In-vessel Components for 1st Plasma

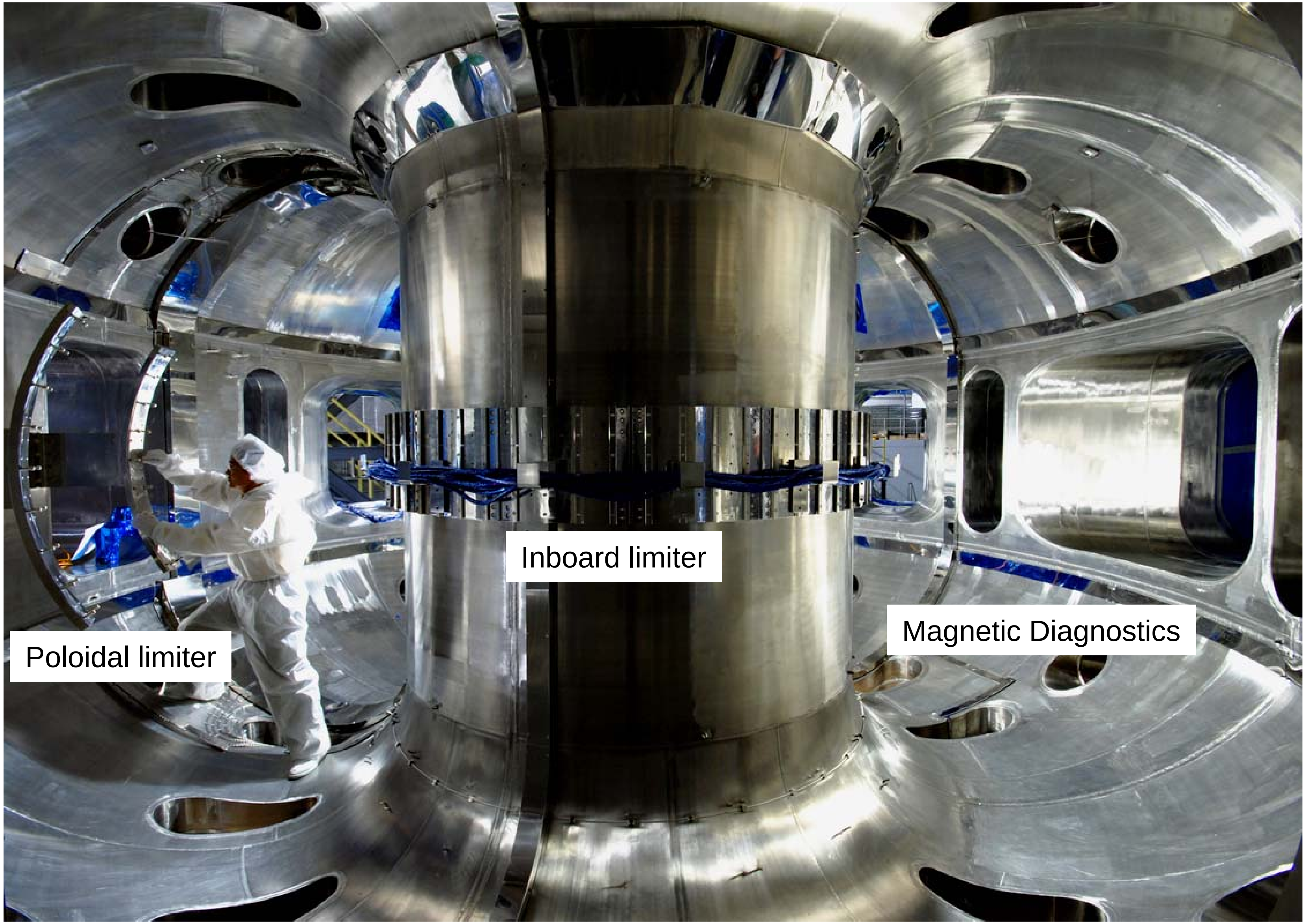

Assessment of ECH 2nd harmonic pre-ionization

First of all, 60GHz and 110GHz experiments are rather confusing in terms of energy growth rate (β) as commented by Dr. England. Therefore, whether it applies to the case of KSTAR 1st plasma is still uncertain.

According to the paper,

$$\beta = 0.5 E_0 k_0 / B_t \propto P^{1/2} / d_{beam} \,,$$

$$d_{beam} \sim d_0 \left[1 + \left(2x_a / k d_0^2 \right)^2 \right]^{1/2} \sim 2x_a c / \omega_{ECH} d_0$$

For KSTAR, x_a~0.5m, k=2π/λ=2 π f/c=1.7e3[1/m], d_0=0.322*63.5mm,

$$\beta = 0.5 E_0 k_0 / B_t \propto P^{1/2} / d_{beam} k_0 / B_t \,,$$

$$d_0 \left[1 + \left(2x_a / k d_0^2 \right)^2 \right]^{1/2} \sim 0.35 > 2x_a c / \omega_{ECH} d_0 \sim 0.28$$

so, there are 20% different !!

$$\frac{\beta_{KSTAR}}{\beta_{DIII-D,60GHz}} = \left(\frac{P_{KSTAR}}{P_{DIII-D}} \right)^{1/2} \frac{d_{beam,DIII-D}}{d_{beam,KSTAR}}$$

$$= (450/400)^{1/2} \times 0.170 / 0.035 = 3.68$$

$$\frac{\beta_{KSTAR}}{\beta_{DIII-D,110GHz}} = \left(\frac{P_{KSTAR}}{P_{DIII-D}} \right)^{1/2} \frac{d_{beam,DIII-D}}{d_{beam,KSTAR}}$$

$$= (450/400)^{1/2} \times 0.034 / 0.035 = 0.75$$

Lower ratio for 60GHz!!

We may decrease the distance(x_a) of the 2nd harmonic resonance layer from the waveguide to decrease d_{beam}
(ratio of beta will be easily larger than 1, so it will be good news for KSTAR!,
e.g., B_t~1.7T->R=1.9m, x_a~0.3m, beta ratio~1 : LFS breakdown)

The results are encouraging, however, above calculations are for electron perpendicular energy growth rate only (1st phase). Avalanche criteria(2nd phase) is not assessed at all for 2nd harmonic ECH heated plasma!
Also, connection length L will be uncertain for KSTAR initially(<1000m, probably less than DIII-D) !

Therefore, it seems we don't have the decisive experimental data and the theoretical model to judge ECH pre-ionization capability for KSTAR 1st plasma. (it will decrease the required loop voltage somewhat, at least, when synergy of V_{loop} & ECH is successful)

GDC Operational Parameters

- S_P/A : 0.1m/s
  - A : 80m^2 (7% of A_{vac})
  - S_P : 8,000 l/s
- the ratio of the pump speed to the effective area of the wall.
- T_W : >150℃ (if possible)
- the wall temperature.
- j_{GD} : 10-25μA/cm^2
- the glow discharge current density.
- P_{H2} : 3 x10^{-3}torr
- the hydrogen pressure.
- Q_{in} : 24 torr l/s (~2000sccm)
- Gas feeding rate.

GDC :Concept of RF assisted DC Glow

- RF assisted DC glow discharge
  - Low ignition, low sustain pressure
  - No ignition circuit
  - Low RF power
  - Large pumping speed
  - Complex structure

  - Mechanical arrangement of the RFX GDC system

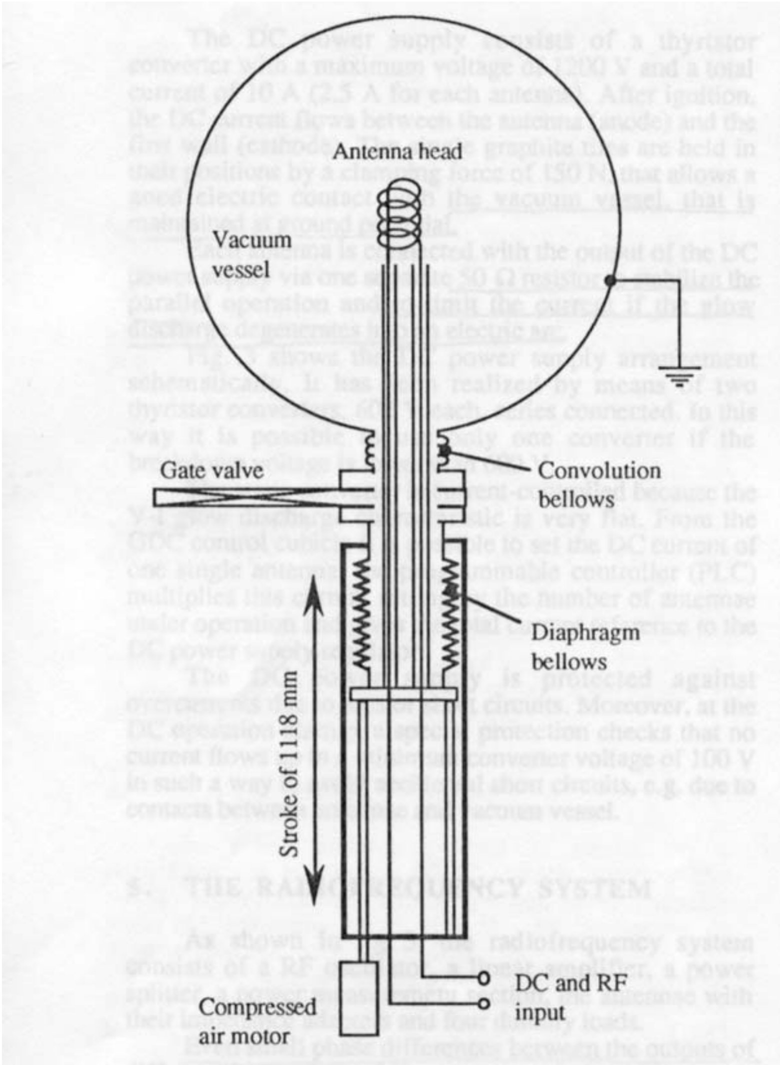

GDC :Conceptual View of Electrode

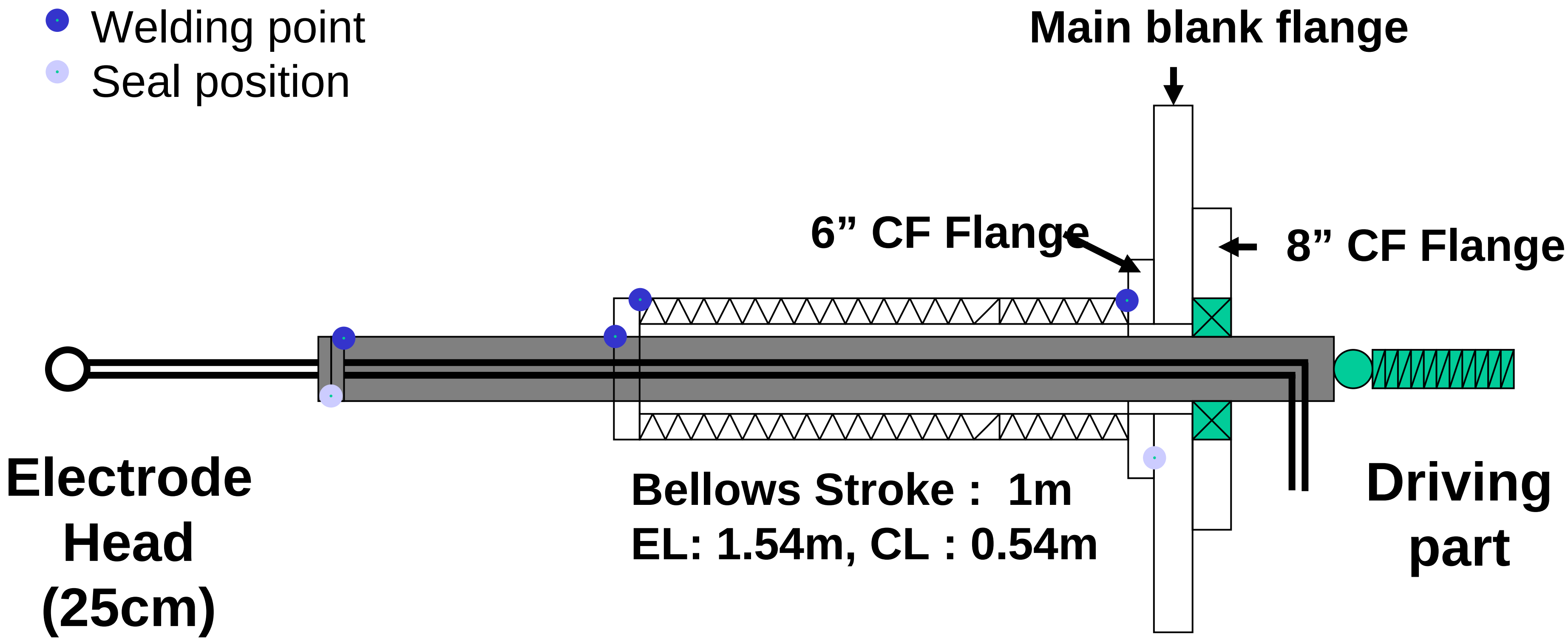

Body (power, cooling lines)
Length : ~3m
Dia. : 70mm

Plasma Initiation Modeling

- 0-D plasma startup model
- 1.2x10^{-5} torr hydrogen pre-fill
- 150 kW absorption of assisted power using ECH 2nd harmonic pre-ionization

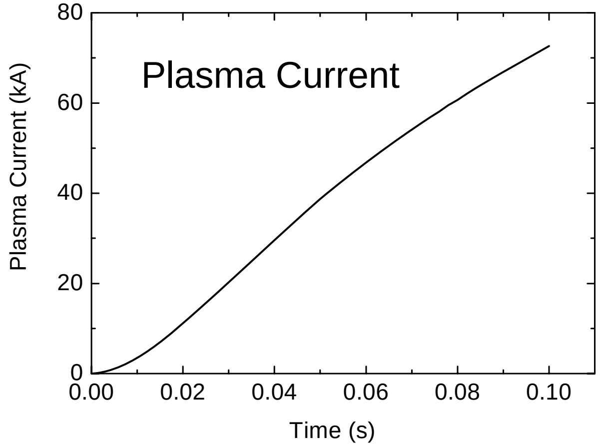

0.72 MA/s of plasma current ramp-up

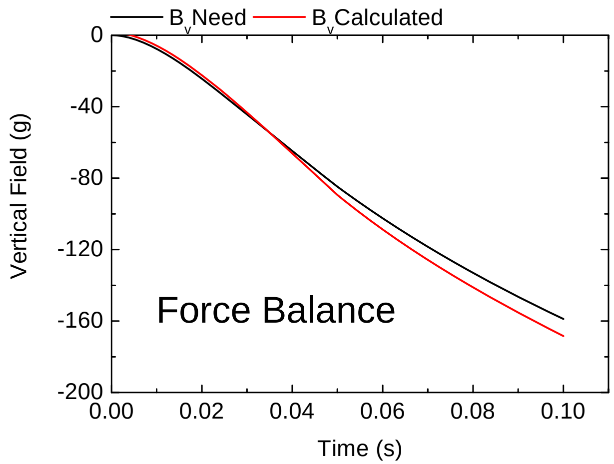

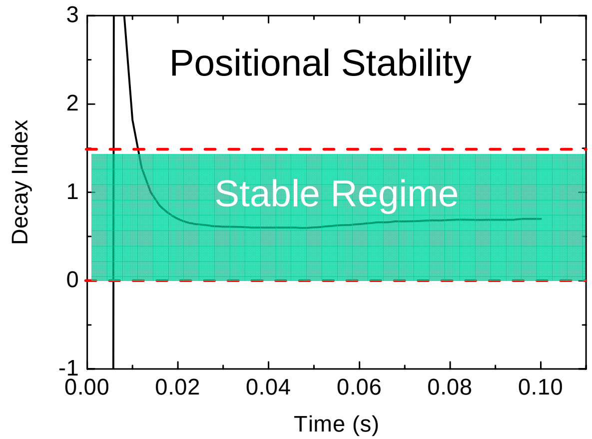

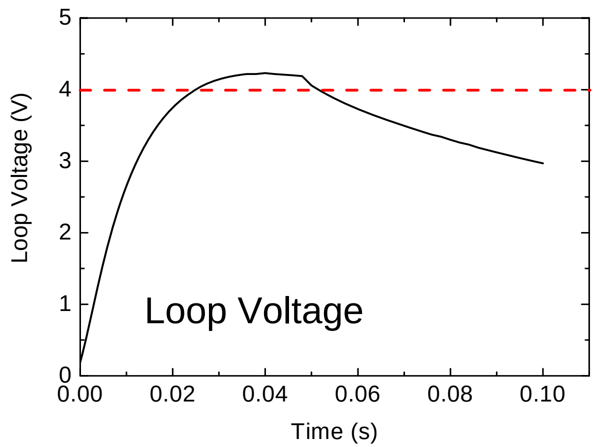

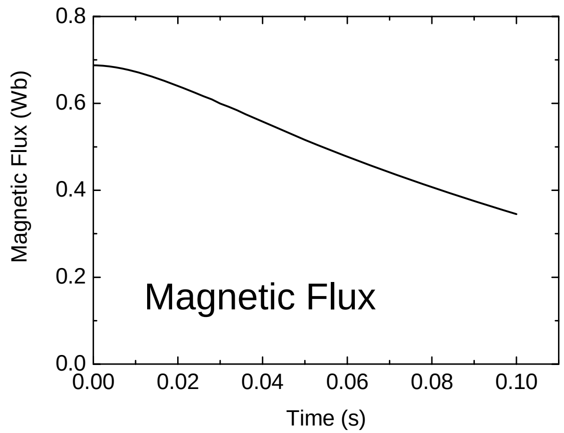

Initial magnetization Analysis

- PF current ~ 10kA in total, magnetization flux ~ 0.7 wb
- Breakdown radius ~ 10cm, residual vertical field ~ 2-4 G

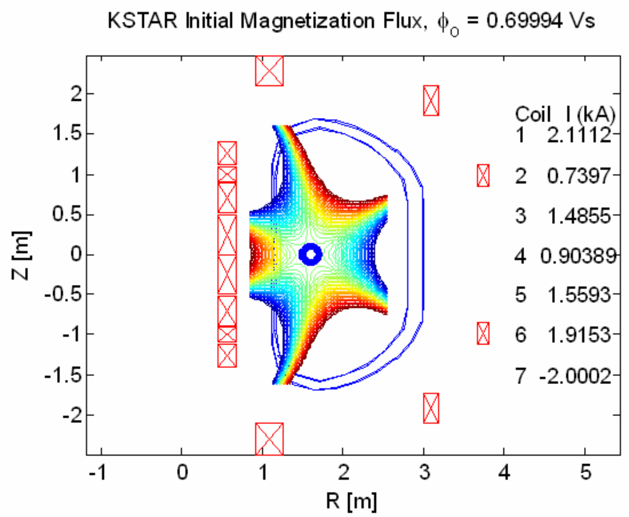

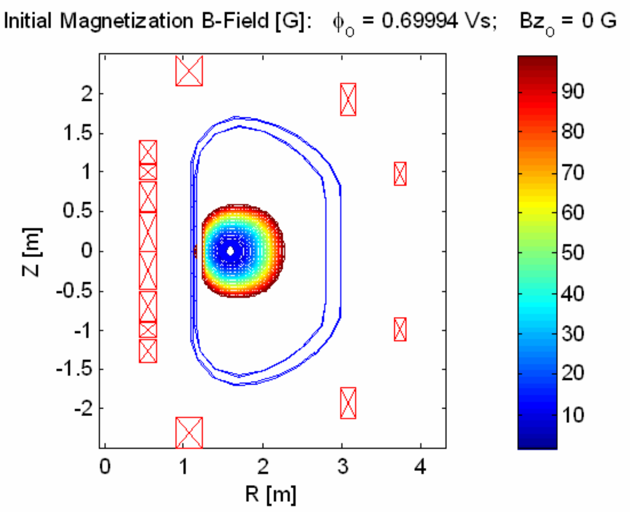

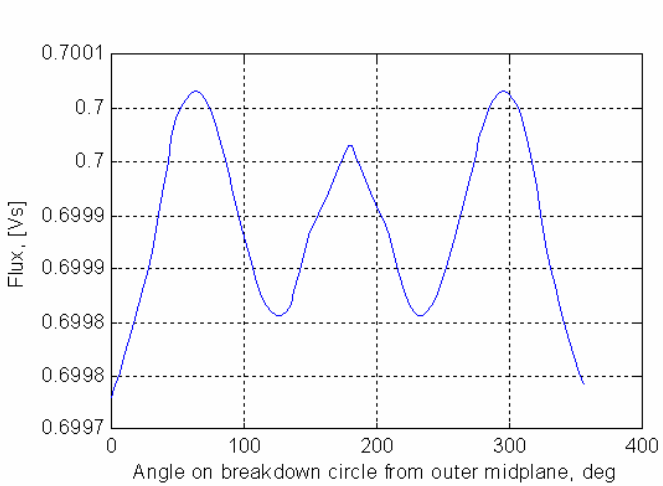

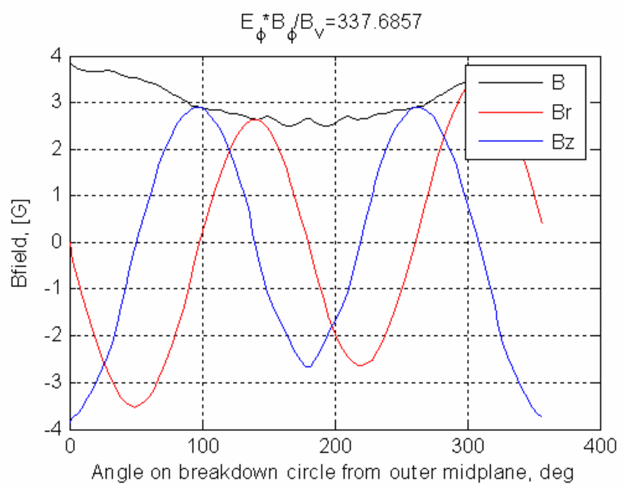

Design and tile temperature calculations for 20s pulse phase

Plasma Facing Components

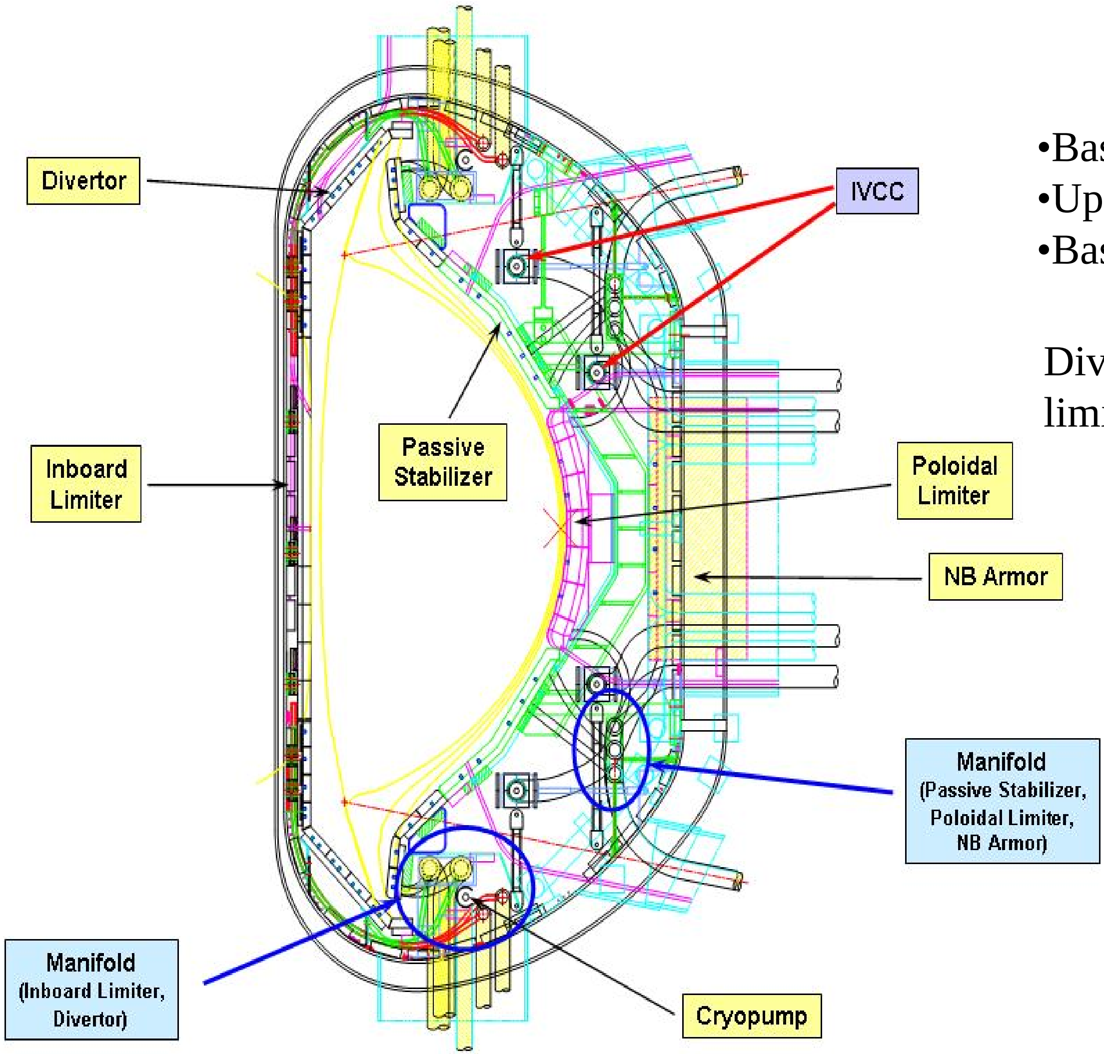

- Based on TPX design
- Up-down symmetric divertor
- Basically major PFC covered by **Graphite**

Divertor, NBI shine-though, and poloidal limiter are covered by **CFC**

Wall gap at the midplane is about 2cm for stability concern

Density control is mainly done by feedback control of gaspuff and outer striking points

Design of PFCs and Heat Removal

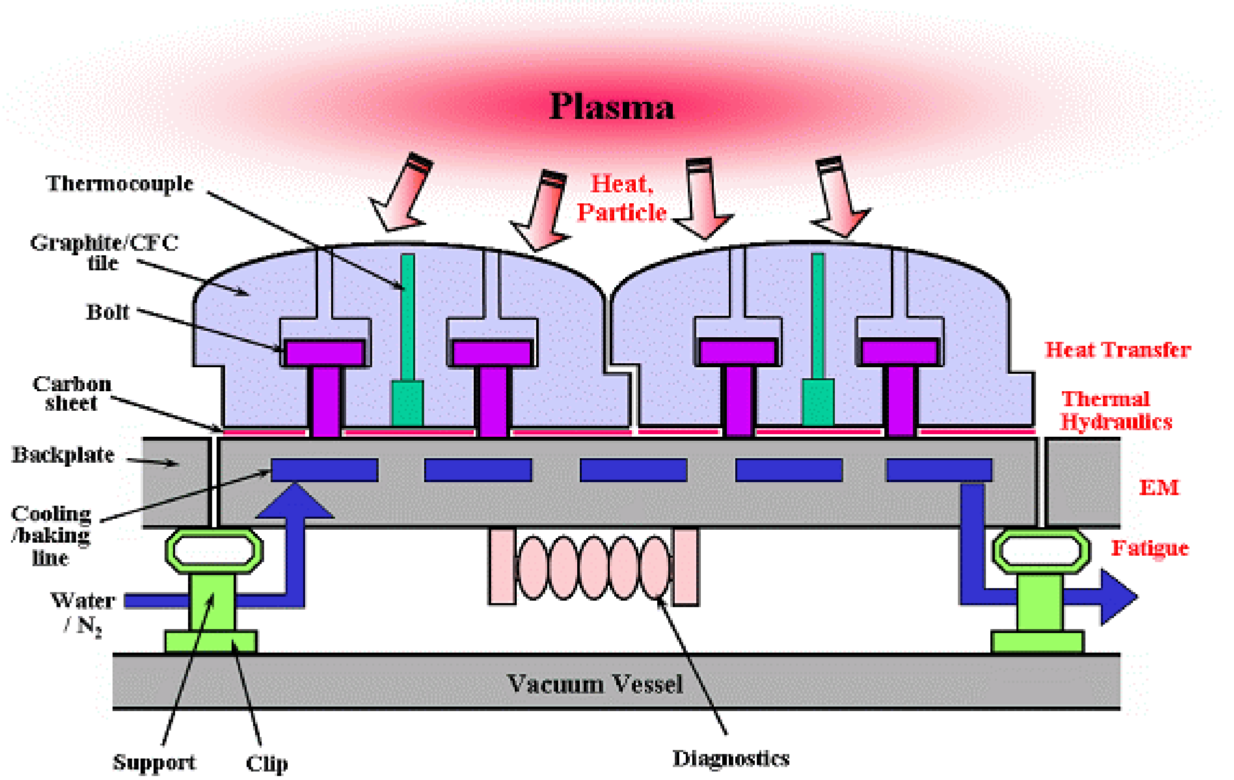

Heat Removal Modeling

$$\rho C(T)\frac{\partial T}{\partial t}-\nabla\cdot\left(\kappa(T)\nabla T\right)=0$$

Boundary conditions
Neuman (q=0) everywhere except for
Tile surface : heat flux(~ MW/m^2)
Coolant : $q=h(T-T_{ext})$

2-D model

Limitation of 2-D

***Constant material properties at 323K**

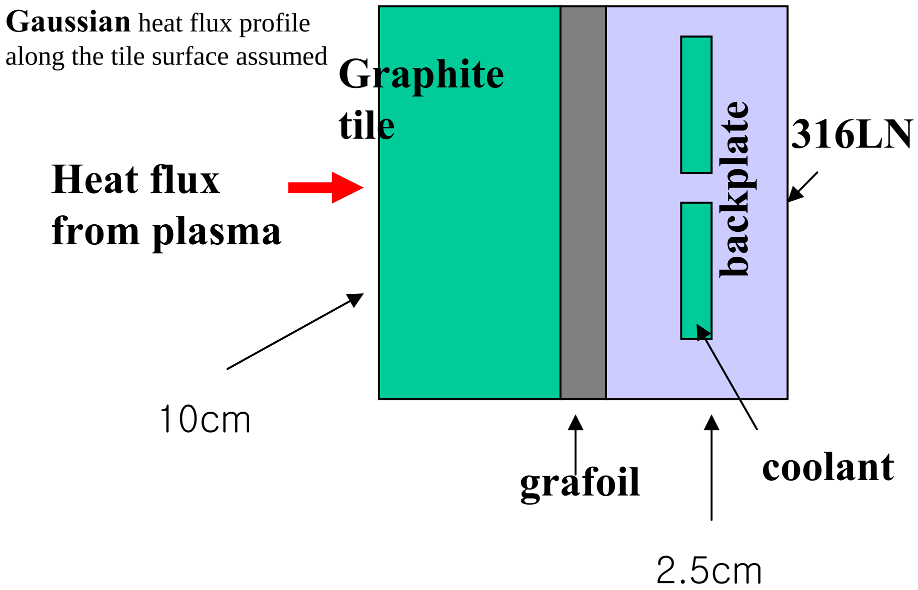

Time dependent
FEM (Matlab PDE solver)

1-D model

***Temperature dependent material properties for tile and backplate**

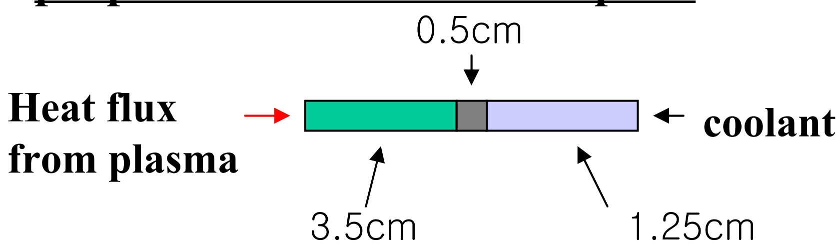

Time dependent
FDM (Matlab PDE solver)

Coolant h=0.25 W/cm^2-C
Grafoil conductance K=0.4 W/cm^2-C
(Due to computational concerns,
Grafoil thickness is enlarged artificially)

Benchmark with the previous 1-D calculations

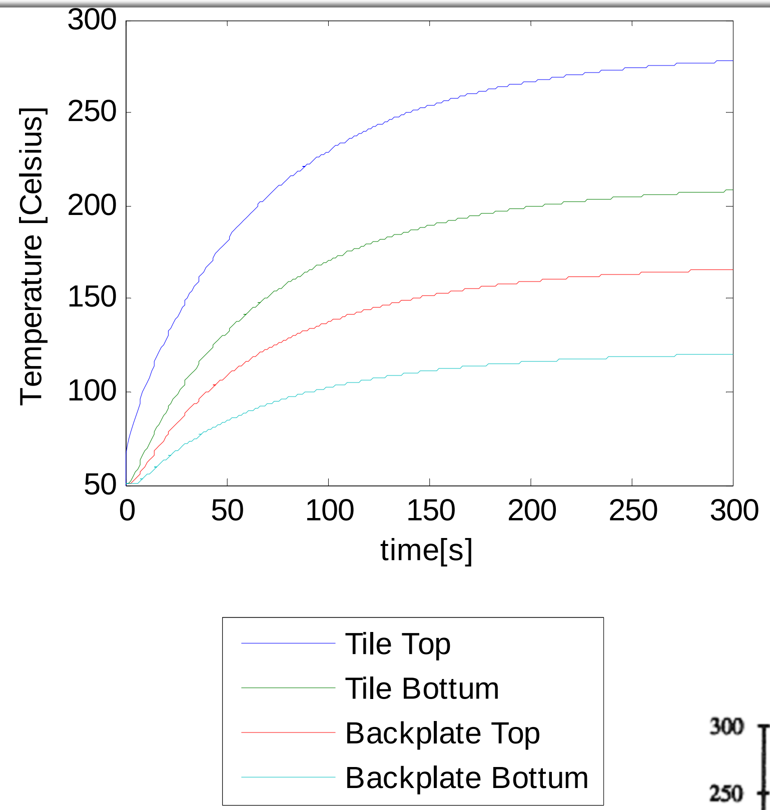

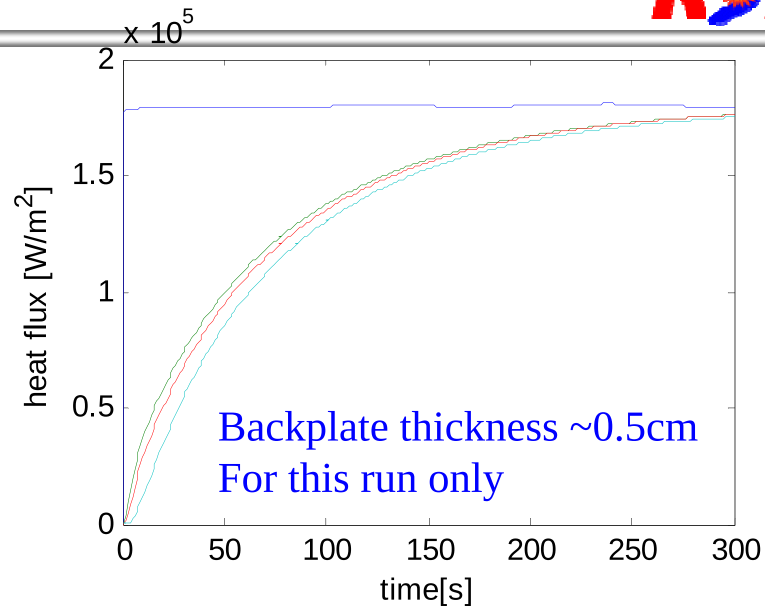

Temperature dependent coefficients for tile and backplate are used
=> Amazingly very similar !
(due to the interplay of conductance and heat capacity)

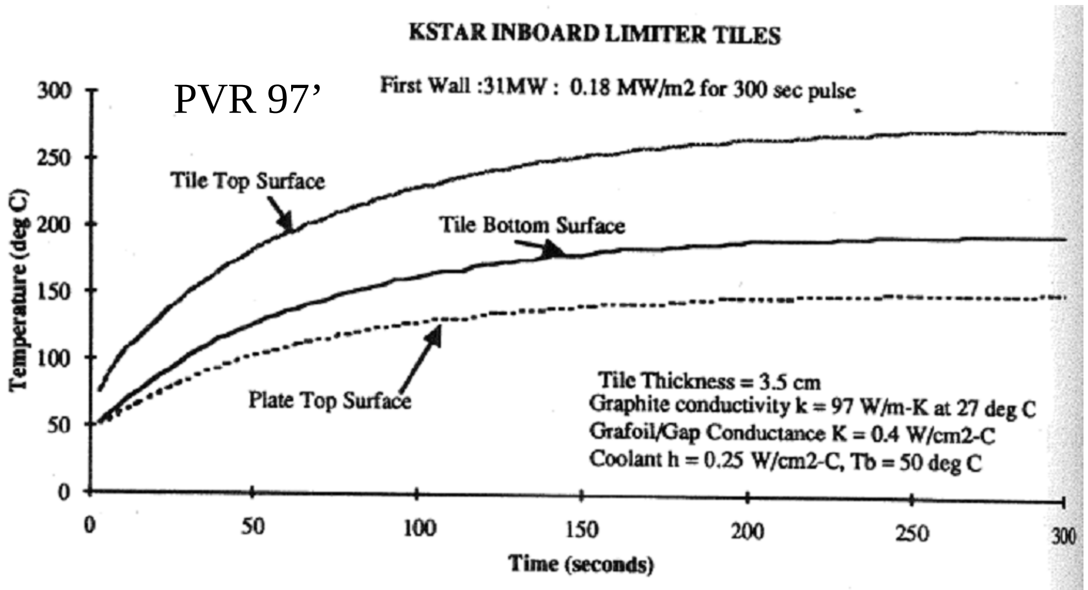

Fig. III-D-3-2. Thermal response of inboard limiter tiles.

Material Thermal Properties

$$\rho C(T)\frac{\partial T}{\partial t} - \nabla \cdot \left(\kappa(T) \nabla T \right) = 0$$

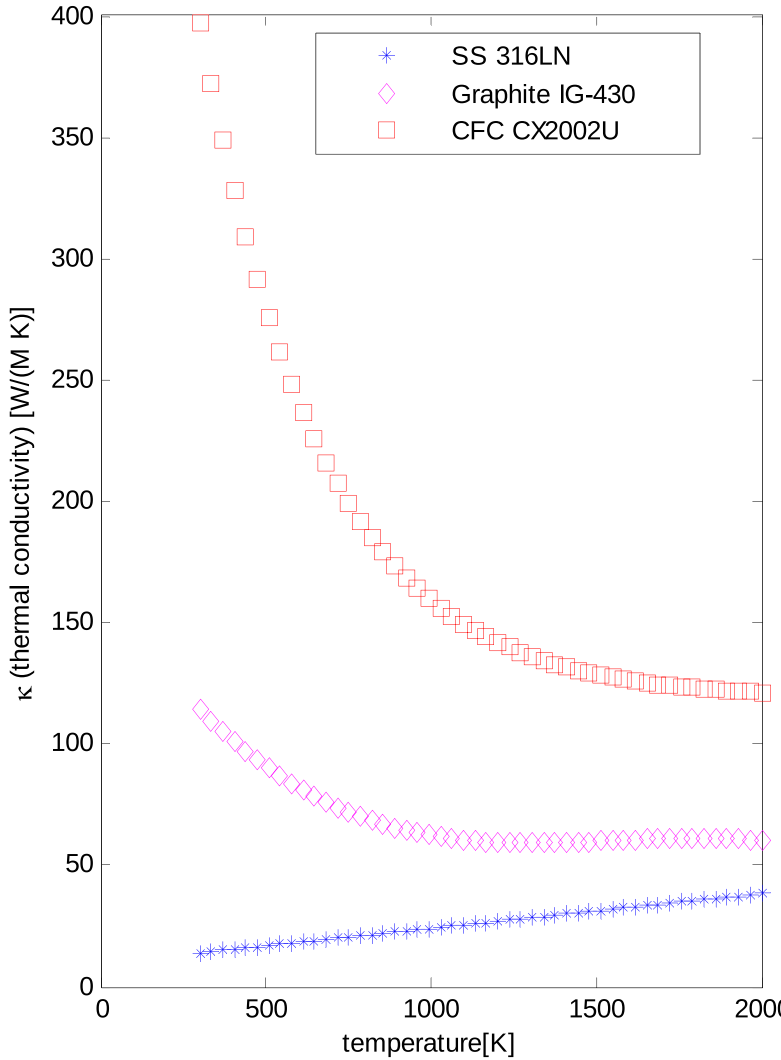

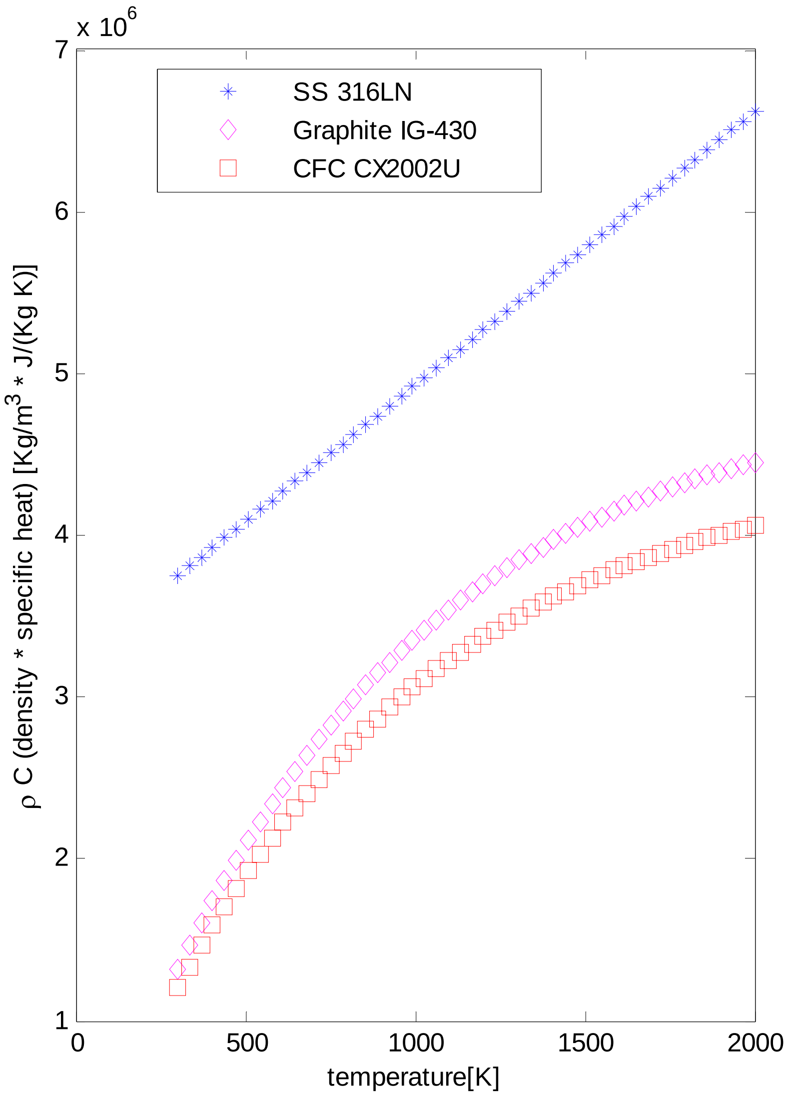

Benchmark : Comparison with 1-D and 2-D calculations

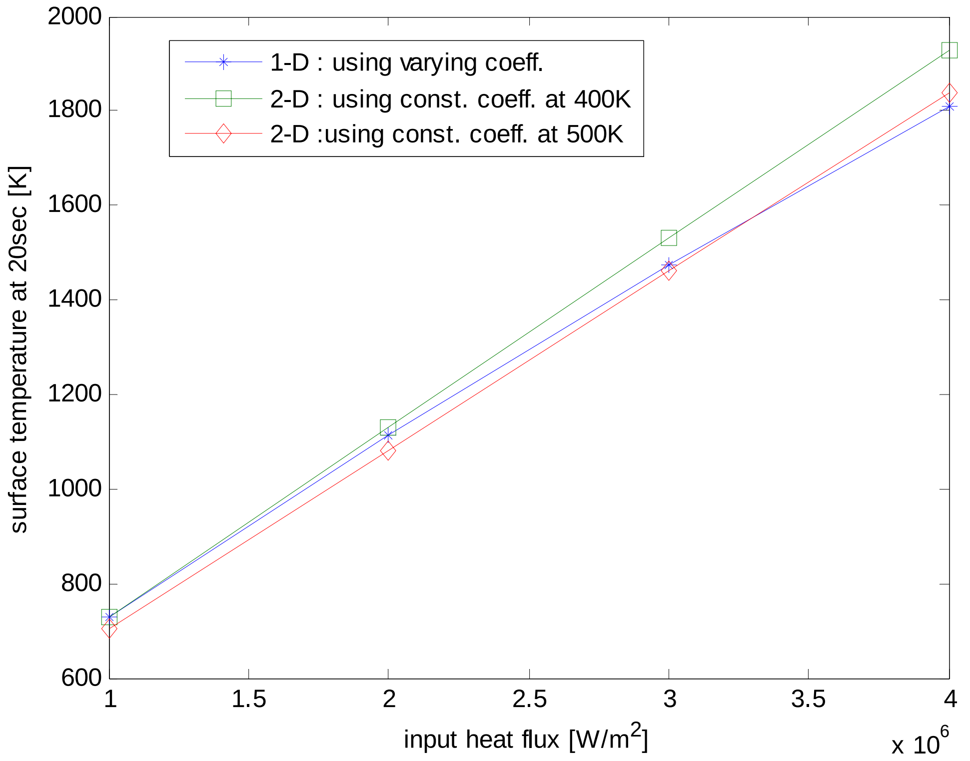

Discrepancy are within 10%!

So for 1-D : varying coefficients

for 2-D : constant coefficients at 450K

are used….

Example of 2-D calculation

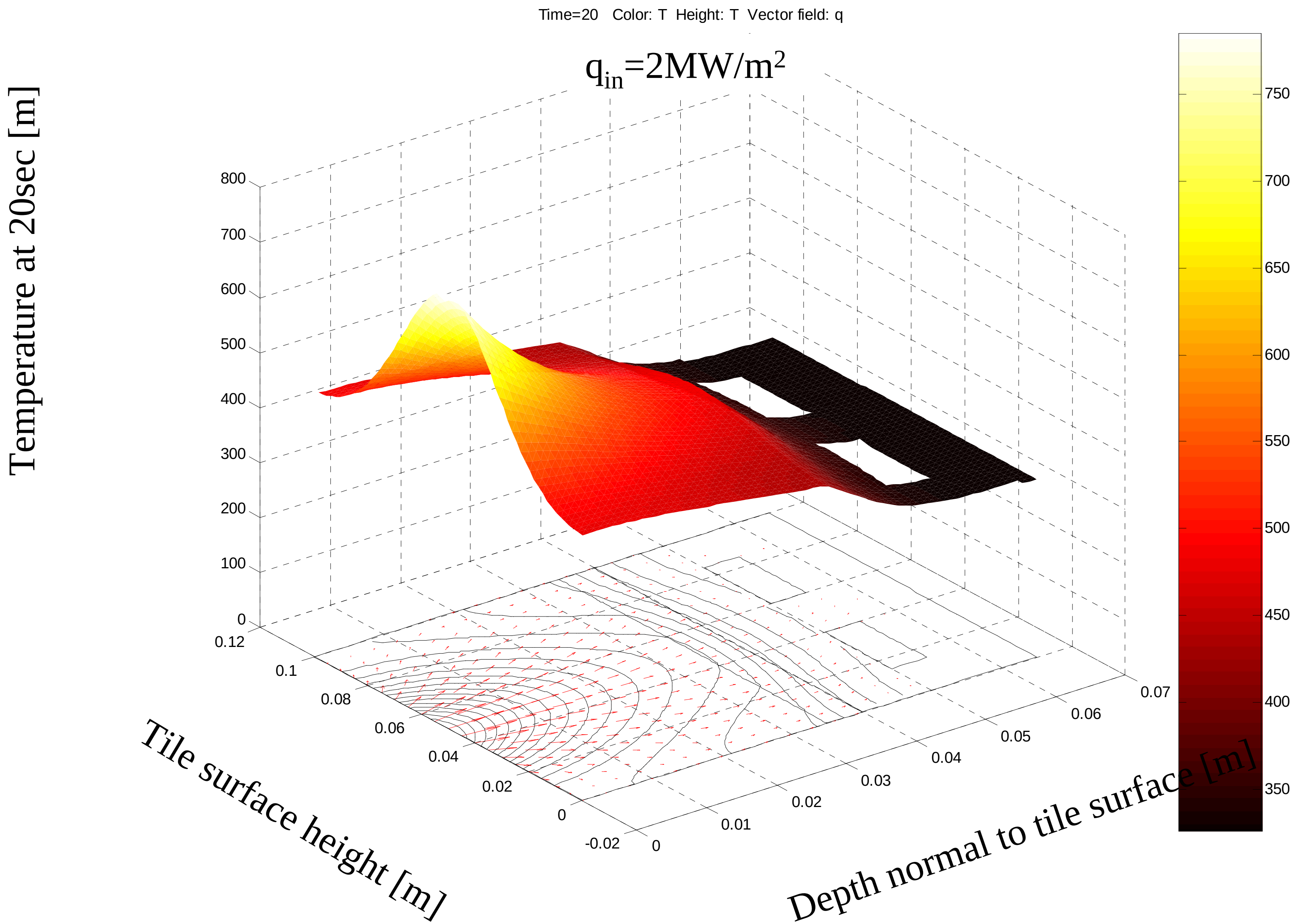

2-D : dependence of tile temperature on heat flux profile

$$q_{in} = q_{\max} \exp(-((y-a)/0.02)^2)$$

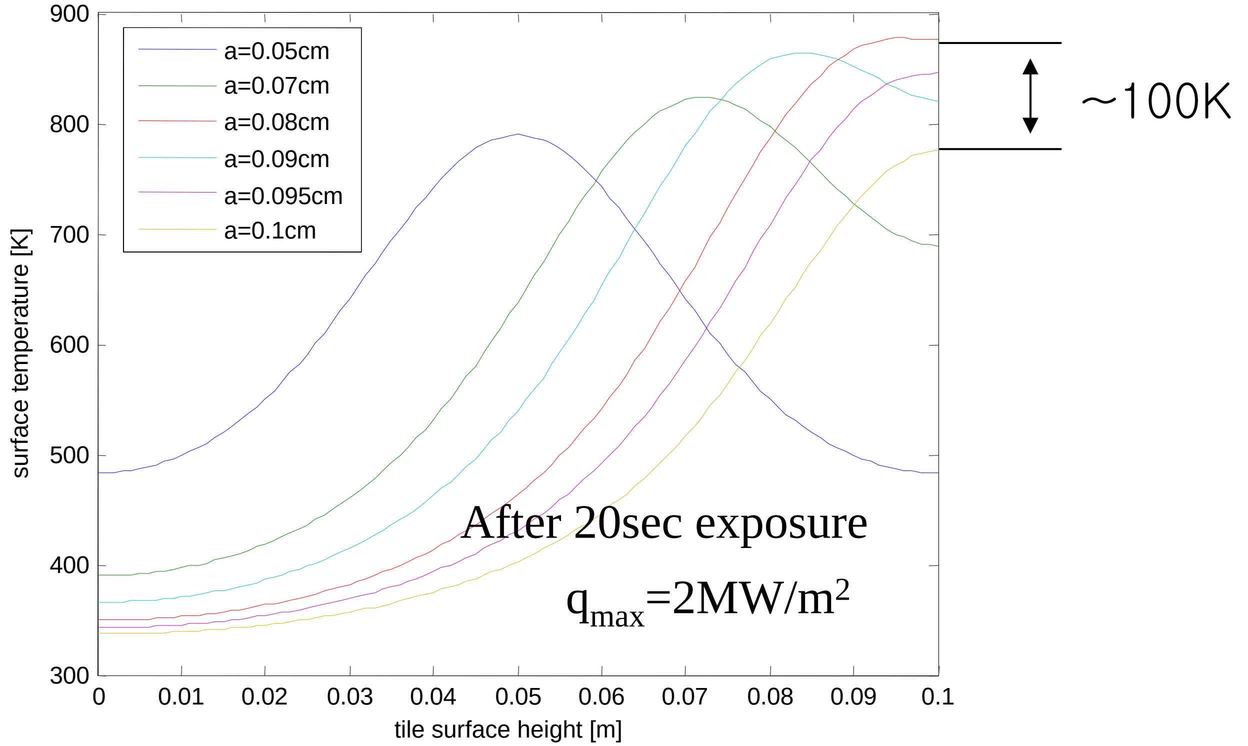

As the peak move sideway, max. temperature increases.
(it returns to the original when x=0.01cm)
However, for divertor, heat flux profile is more like triangular rather than guassian
=> the case of x=0.05cm is a good guess for standard operation!

2-D calculations of tile temperature after 20sec exposure

KSTAR

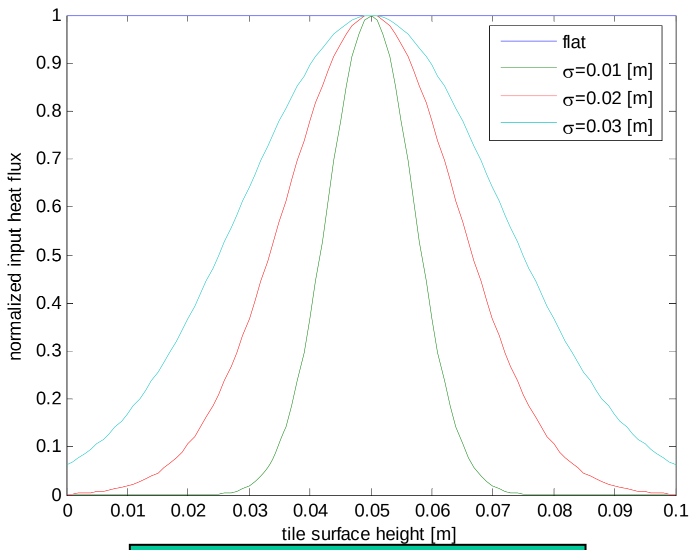

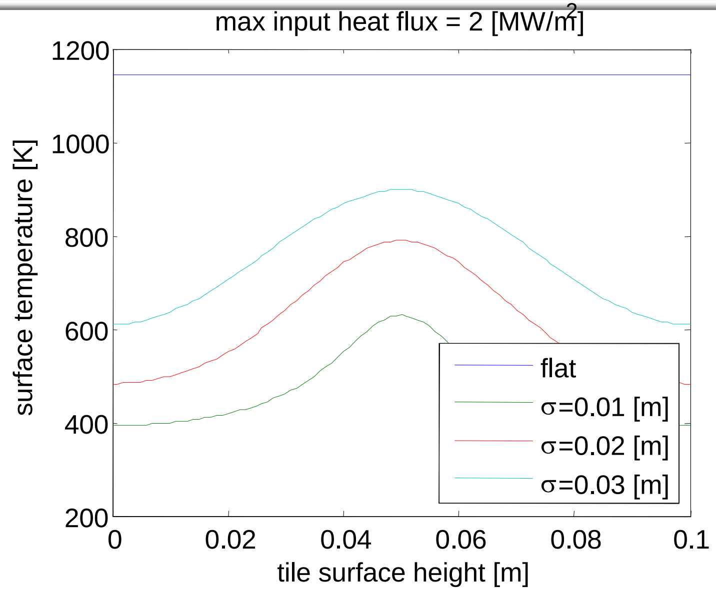

$$q_{in} = q_{\max} \exp(-((y-0.05)/\sigma)^2)$$

Estimated heat flux
for ~6MW = 1.3 MW/m2

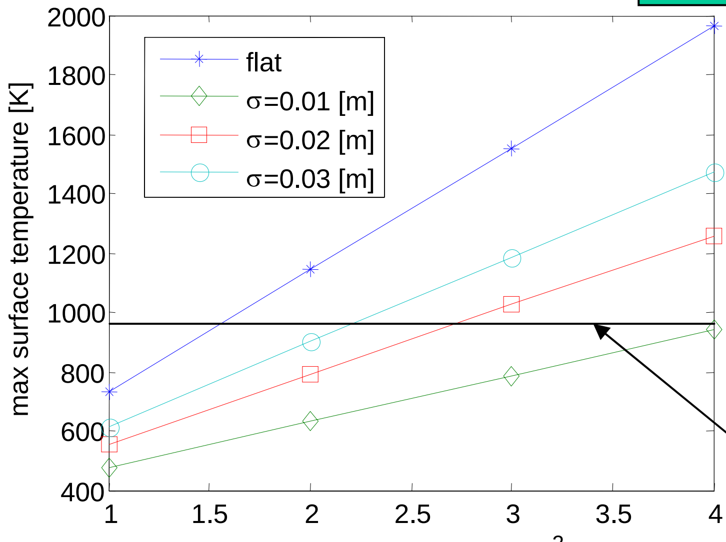

limiting T for graphite

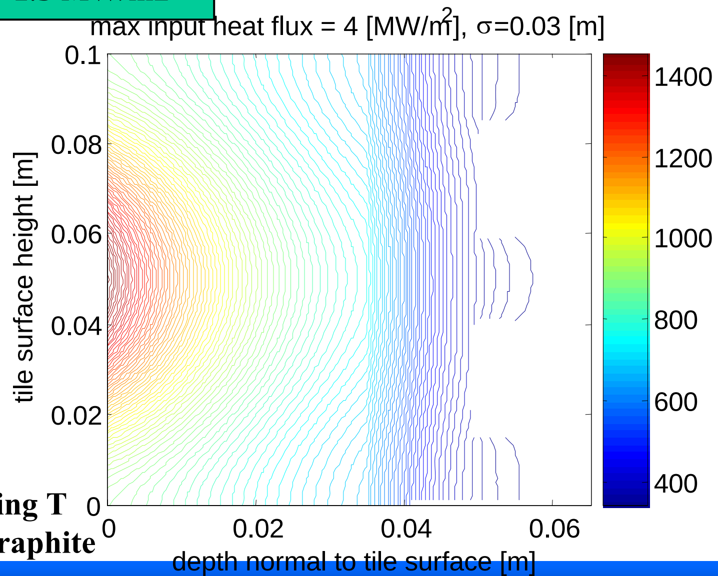

1-D : Effect of active cooling for short pulse(<40sec)

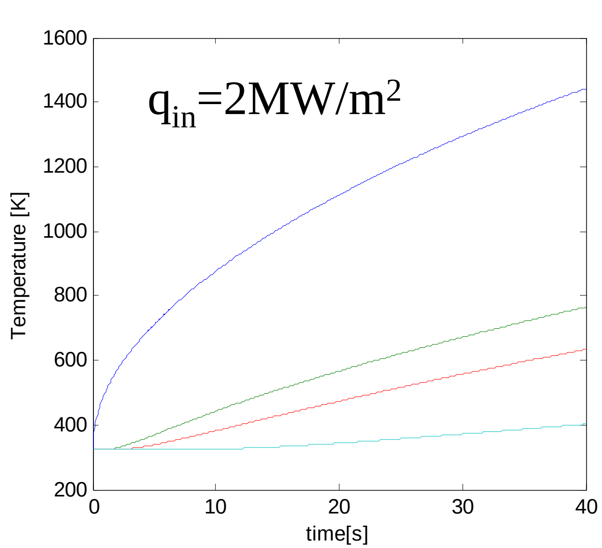

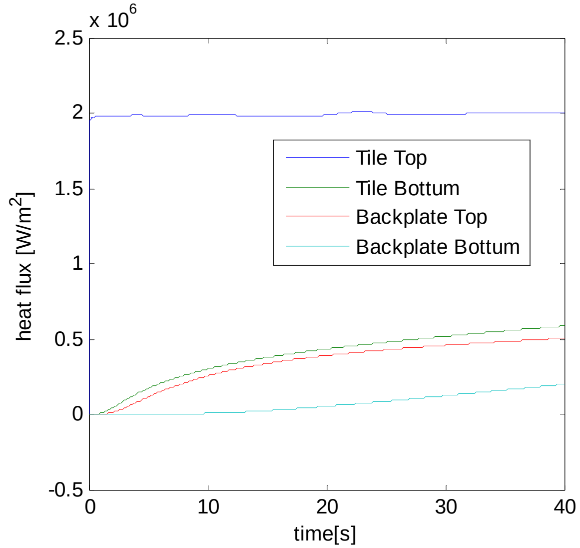

Active cooling on
h=0.25 W/cm^2-C

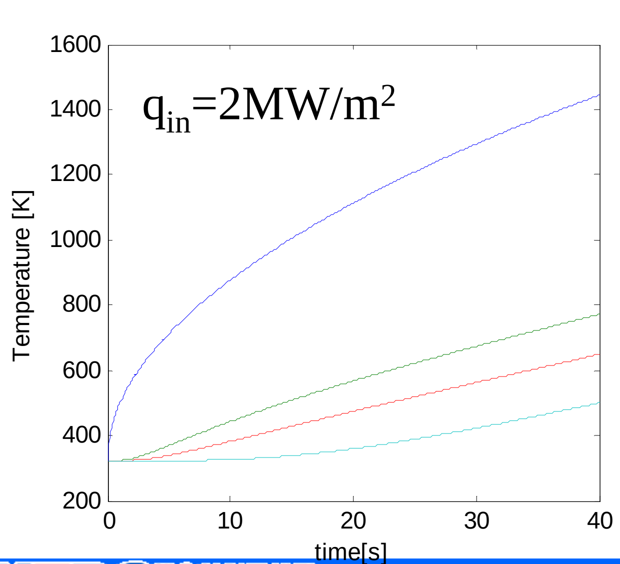

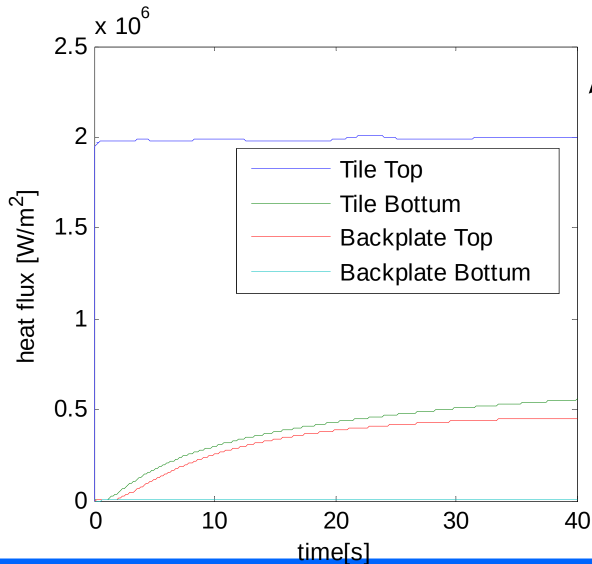

Active cooling off
Neuman condition

at 20sec,
Practically the same T

at 40sec
Surface T is about the same
(backplate increased instead)

1-D Simulation of active cooling time after exposure

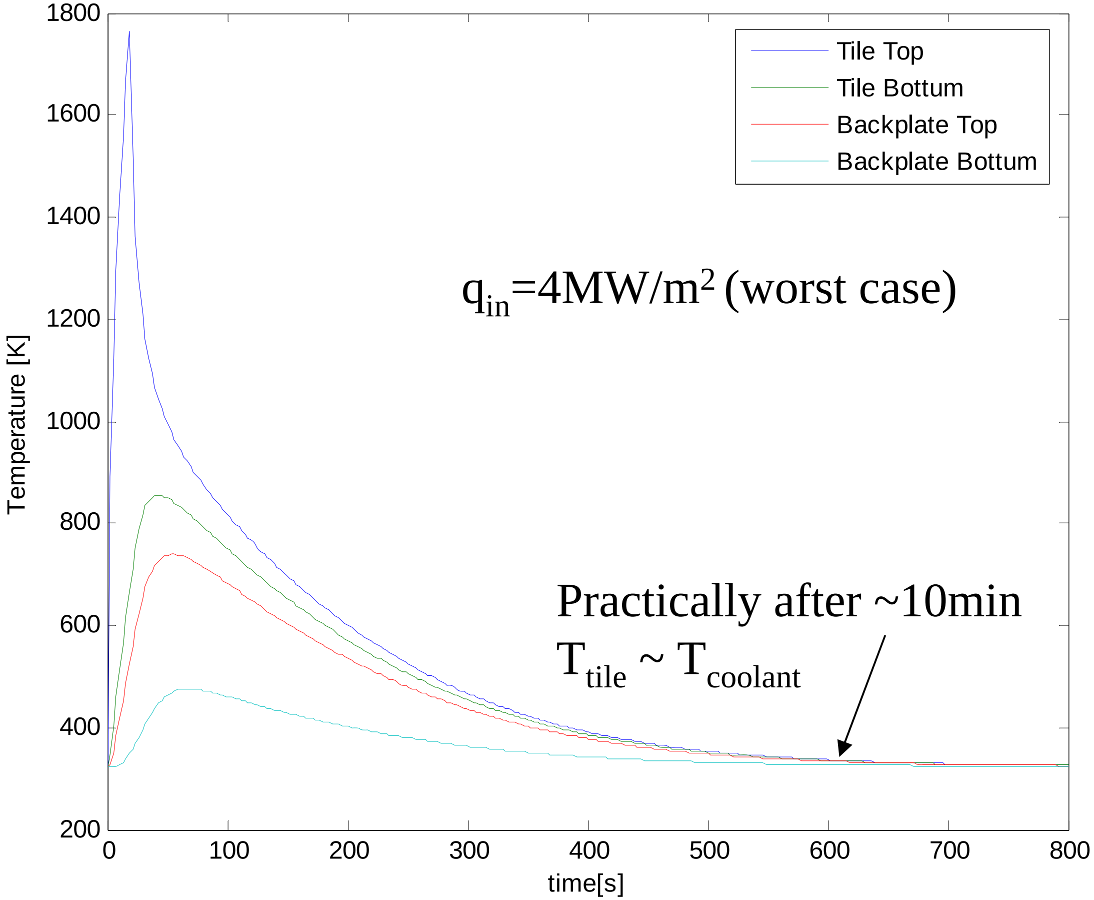

2-D Simulation of striking point modulation for example

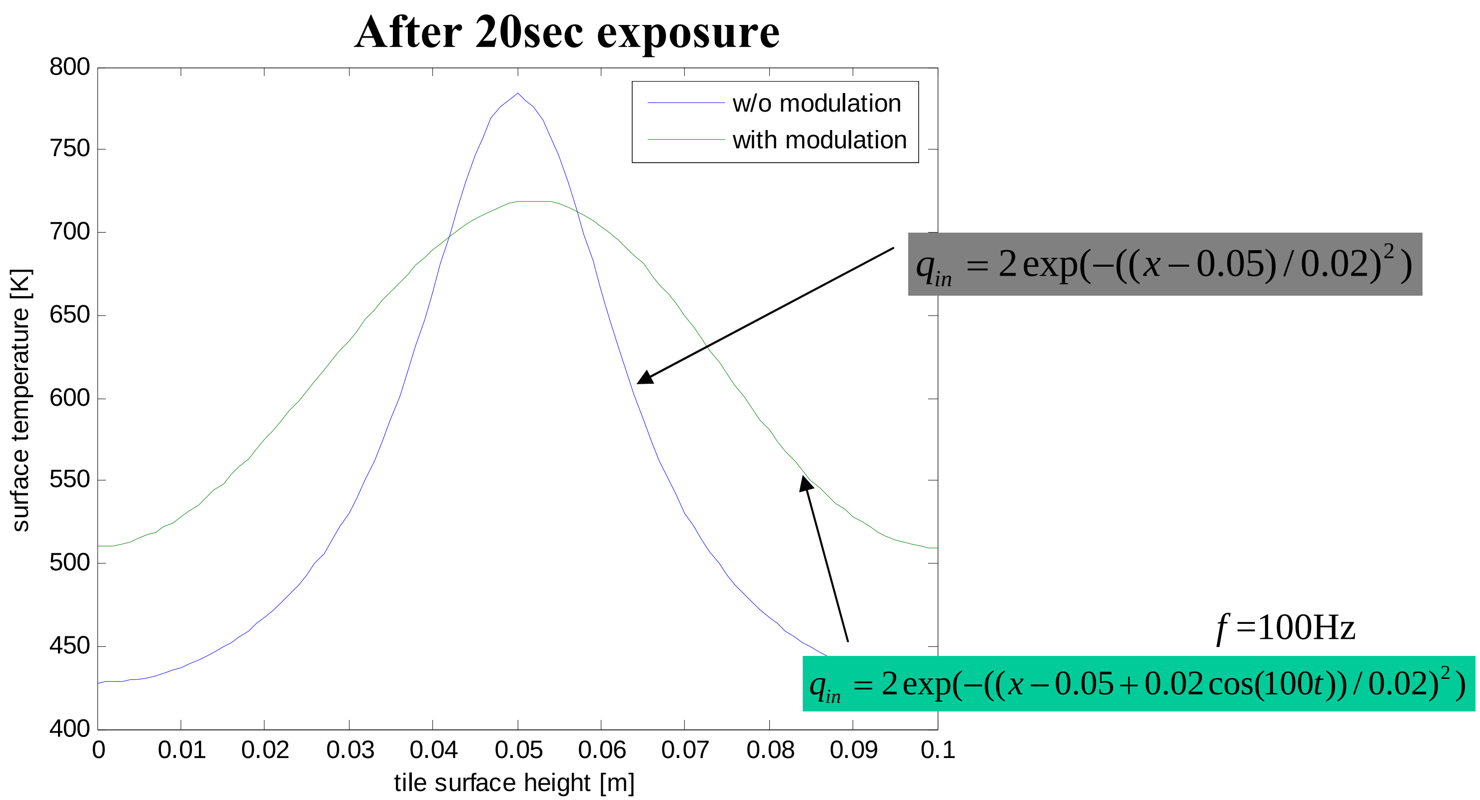

1-D Simulation of tile thickness dependence

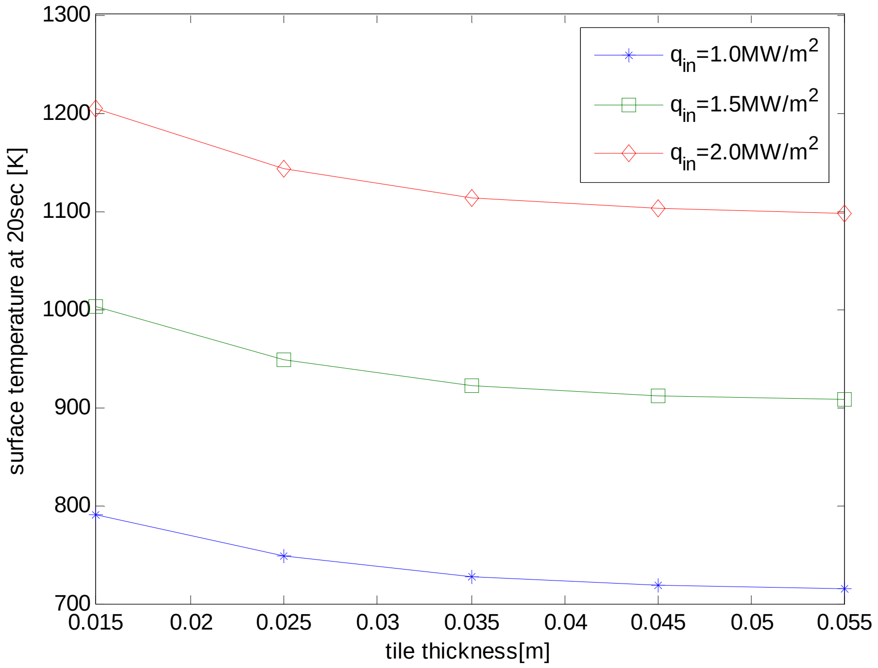

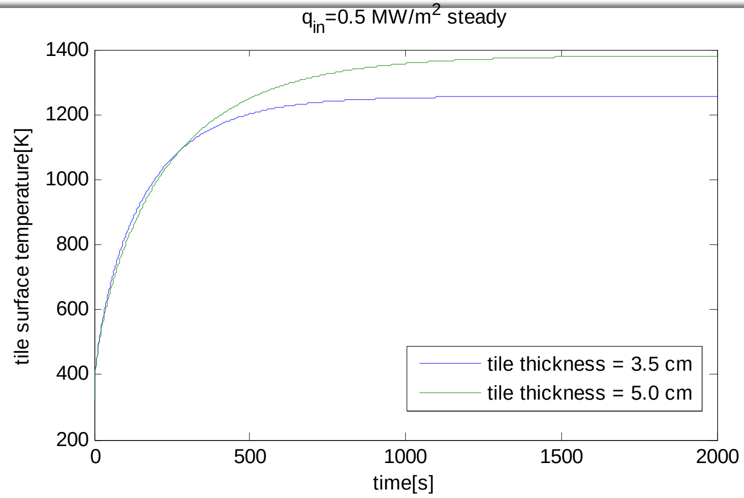

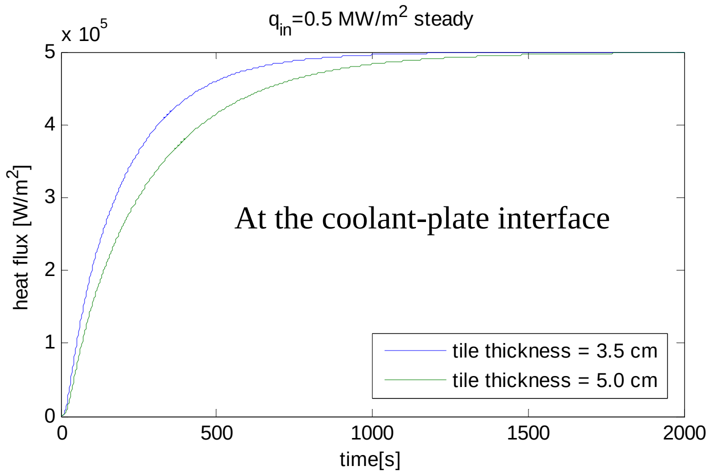

Interesting!
for short pulse(<200~300),
as thickness decreases, T_{surf} increases
(effective conductivity increases!)

for long pulse(>500),
usual behavior recovers!

Conclusion from tile temperature calculations

- For ~6MW+20sec operation,
  graphite is well-suited for power handling with enough safety margin!

  ✓16MW->3.5MW/m^2 -----> 6MW-> 1.3MW/m^2
  ✓In the worst case (flat heat flux profile), q_{limit} ~1.5MW/m^2 (this is not likely at all)
  ✓For normal operation, q_{limit} ~2.5MW/m^2 (e-folding length=2cm)
  ✓Above 3.5MW/m^2 might actually be lower to ~2MW/m^2 (according to DIII-D exp.)

- Variation of tile thickness and striking point sweeping will also help

- Active cooling is not so effective in short-pulse operation <~40sec

- Current cooling design will be sufficient for PFC cooling in-between discharges

Further work needed for:

- 2-D calculations of heat flux from plasma
- 3-D calculations of temperature (including radiation loss)
- Structural analysis with graphite divertor

Plan of PFC Upgrade

•The low power 20 second phase, we will use the present design of PFCs.

•However, in the present design, the density control may be not so efficient for long-pulse especially for single-null case due to the lack of inboard side cryo-pump.

•For high power 300 second phase, the divertor tile will be changed to CFC and brazing will be used between tiles and stainless steel backplates for better heat conduction.

•We are considering W-shape closed divertor with V-shape striking point modules for the long-pulse experiments.

•Also, during short pulse phase, we will test the various PFC materials including W in the dedicated toroidal sector.

Edge transport modeling activities with SOLPS5.0(B2.5)

Computational domain

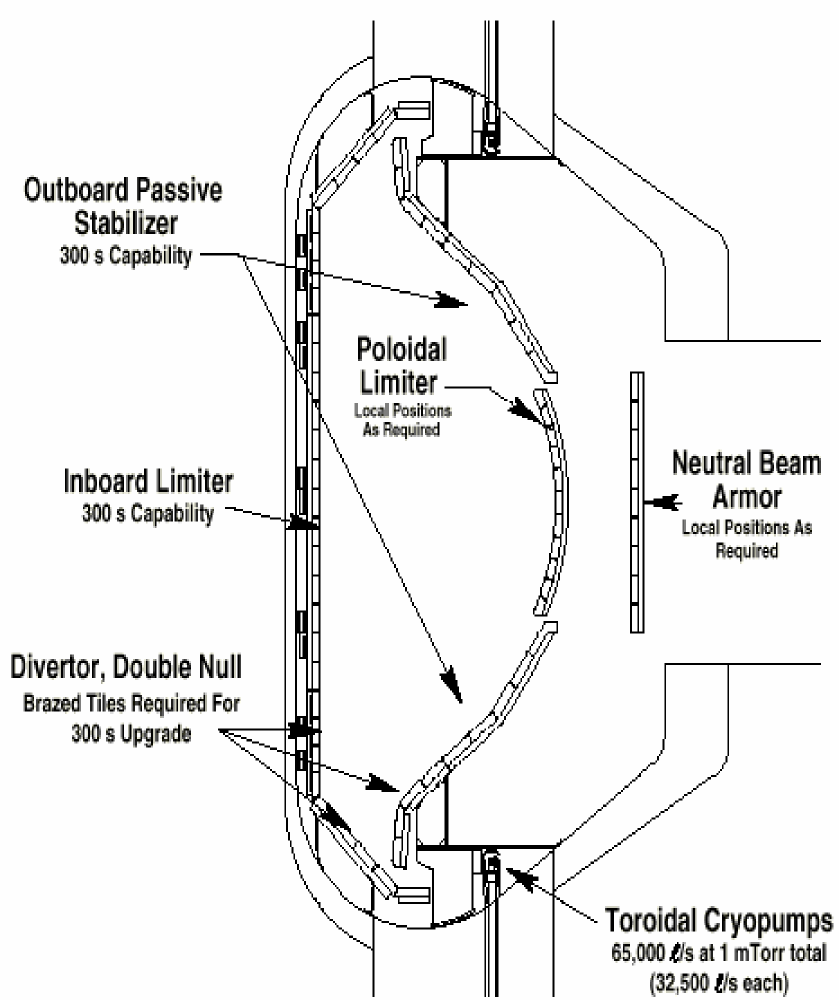

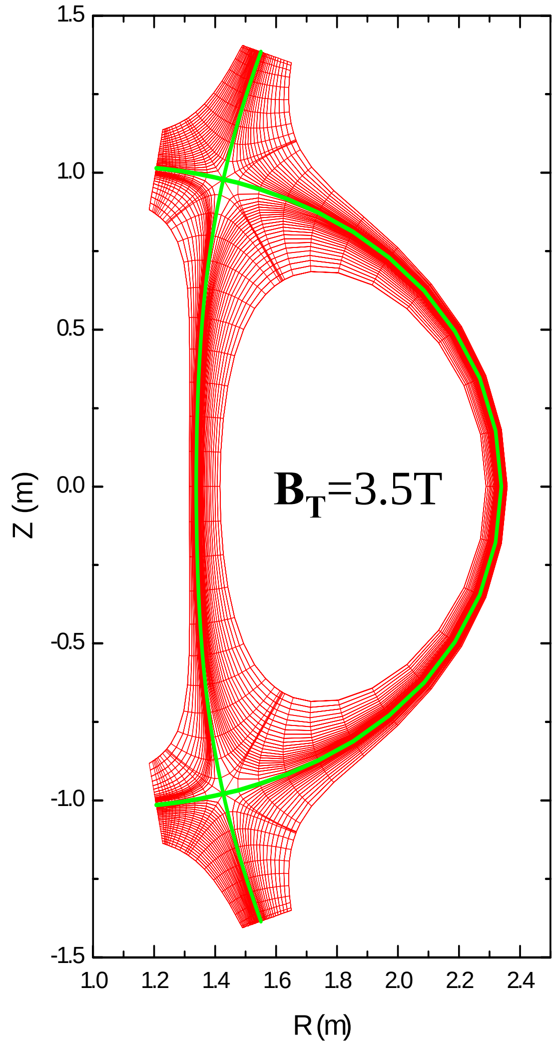

Governing equations

Particle conservation:

$$\frac{\partial n_i}{\partial t} + \nabla \cdot \left(n_i \mathbf{V}_i^{eff} \right) = S_i^n \quad \text{where} \quad \mathbf{V}_i^{eff} = V_{i\parallel}\mathbf{b} + \frac{c}{B}\mathbf{b} \times \nabla \varphi + \frac{cT_i}{Z_i e} \nabla \times \left(\frac{\mathbf{b}}{B} \right) - \frac{D_{an}}{n_i} \nabla_\perp n_i$$

Parallel momentum conservation:

$$m_i \frac{\partial n_i V_{i\parallel}}{\partial t} + \nabla \cdot \left(m_i n_i \mathbf{V}_i^{eff} V_{i\parallel} \right) = -\mathbf{b} \cdot \nabla p_i + Z_i e n_i \mathbf{b} \cdot \nabla \varphi - \mathbf{b} \cdot \nabla \Pi_{i\parallel} + \frac{3}{2} \frac{(\mathbf{b} \cdot \nabla B)}{B} \Pi_{i\parallel} + \nabla \cdot \left(\eta_2 \nabla V_{i\parallel} \right) + S_{i\parallel}^m + F_{ie\parallel}$$

Charge conservation:

$$\nabla \cdot \mathbf{J}^{eff} = 0 \quad \text{where} \quad \mathbf{J}^{eff} = J_\parallel \mathbf{b} + cp \nabla \times \left(\frac{\mathbf{b}}{B} \right) + \mathbf{J}_\perp^{vis+in+s} - \sigma_{an} \nabla \varphi$$

$$\mathbf{J}_\parallel = \sigma_\parallel \left[\frac{1}{e} \left(\frac{1}{n_e} \nabla_\parallel p_e + \frac{\kappa_{12}}{\kappa_{11}} \nabla_\parallel T_e \right) - \nabla_\parallel \varphi \right]$$

Energy conservation:

$$\frac{3}{2}\frac{\partial p_i}{\partial t} + \nabla \cdot \mathbf{q}_i^{eff} = \mathbf{V}_i \cdot \nabla p_i - \mathbf{\Pi}_i : \nabla \mathbf{V}_i + Q_i, \quad \text{where} \ \mathbf{q}_i^{eff} = -\kappa_\parallel^i \nabla_\parallel T_i - \kappa_\perp^i \nabla_\perp T_i - \chi_{an} n_i \nabla T_i + \frac{5}{2} p_i \mathbf{V}_i^{eff}$$

$$\frac{3}{2}\frac{\partial p_e}{\partial t} + \nabla \cdot \mathbf{q}_e^{eff} = \mathbf{V}_e \cdot \nabla p_e + Q_e, \quad \text{where} \ \mathbf{q}_e^{eff} = \frac{\kappa_{12}}{\kappa_{11}} \frac{T_e}{e} J_\parallel \mathbf{b} - \kappa_\parallel^e \nabla_\parallel T_e - \kappa_\perp^e \nabla_\perp T_e - \chi_{an} n_e \nabla T_e + \frac{3}{2} \frac{T_e}{m_e \Omega_e^2 \tau_e} \nabla_\perp p + \frac{5}{2} p_e \mathbf{V}_e^{eff}$$

Simulation conditions (drift-off case)

Simulations were performed at the following various conditions.
For simplicity, we neglected the drift terms.

Parameter	Value
Input power	2~13 MW
Plasma density at core boundary	3~7×10^{19} m^{-3}
Anomalous particle diffusivity D_{an}	0.5 m^2/sec
Anomalous thermal diffusivity χ_{an}	1 m^2/sec
Recycling coefficient at wall and divertor	1.0
Leakage factor in private region by pumping	1~6 %
Decay length at wall boundary	0.02 m

Results at various leakage and density conditions

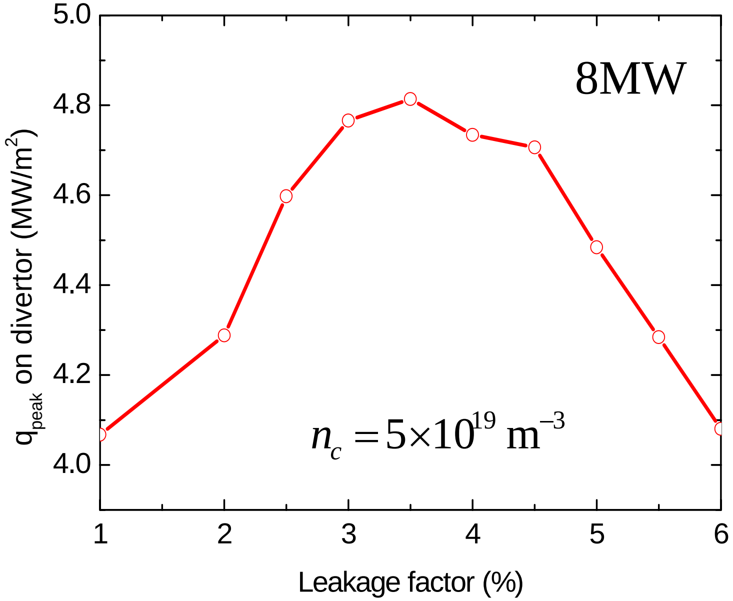

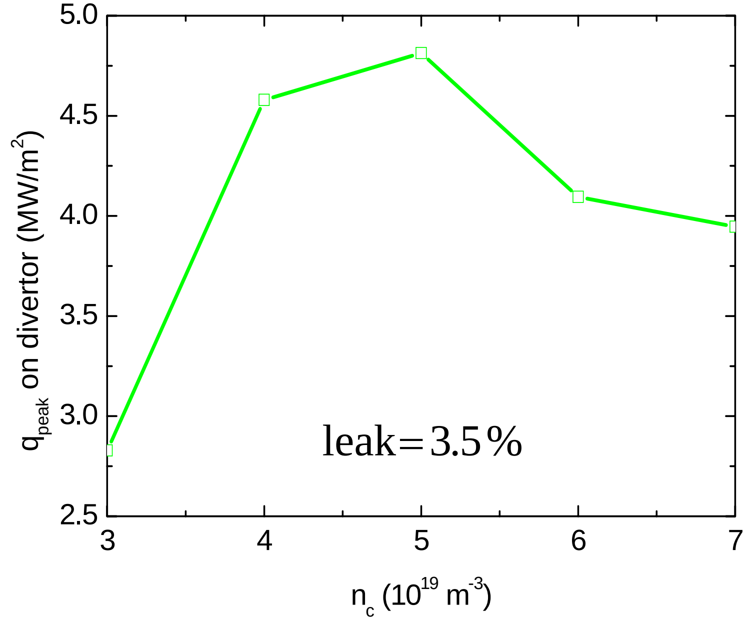

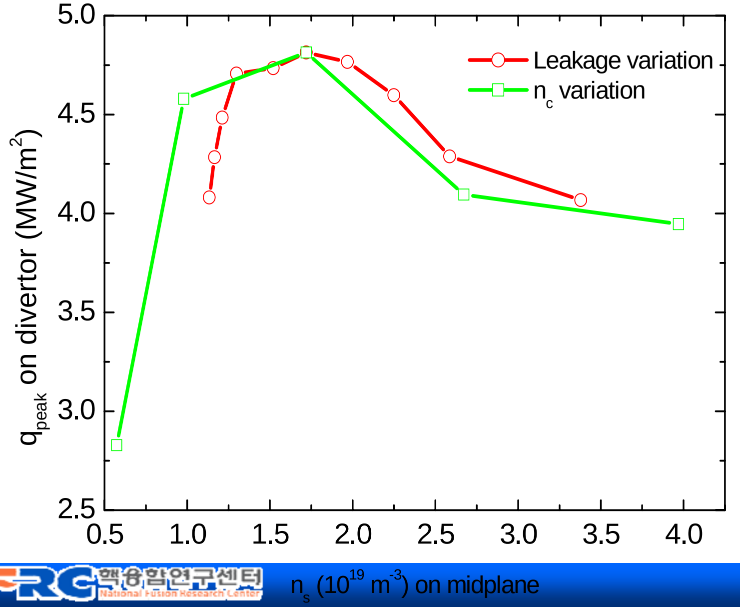

The leakage factor or core density affects midplane plasma conditions, on which divertor heat flux strongly depends.

Similar midplane plasma case at different condition

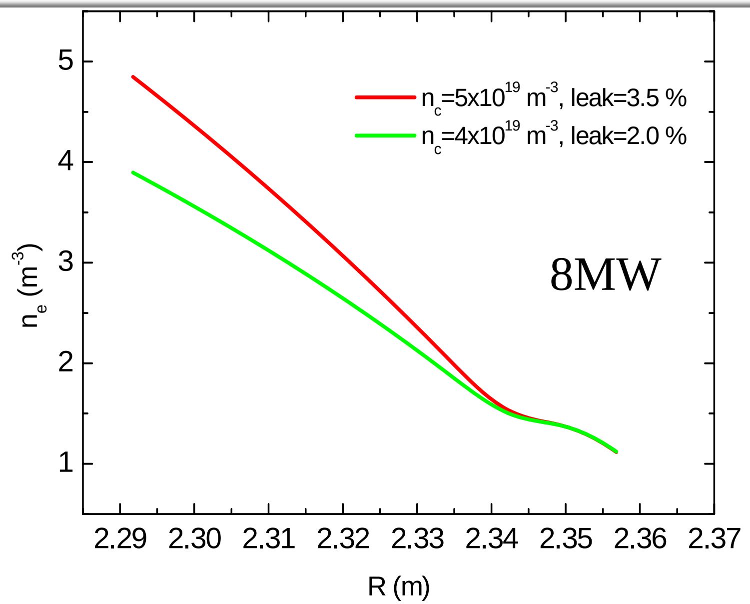

Divertor heat flux is mainly governed by midplane condition: if different combinatio of leakage factor and core density produce similar plasmas on midplane, divertor heat fluxes are also similar.

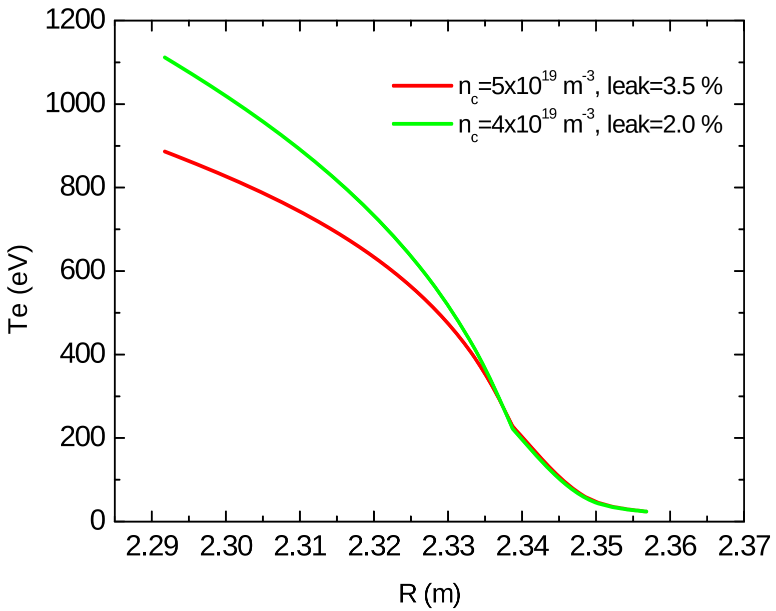

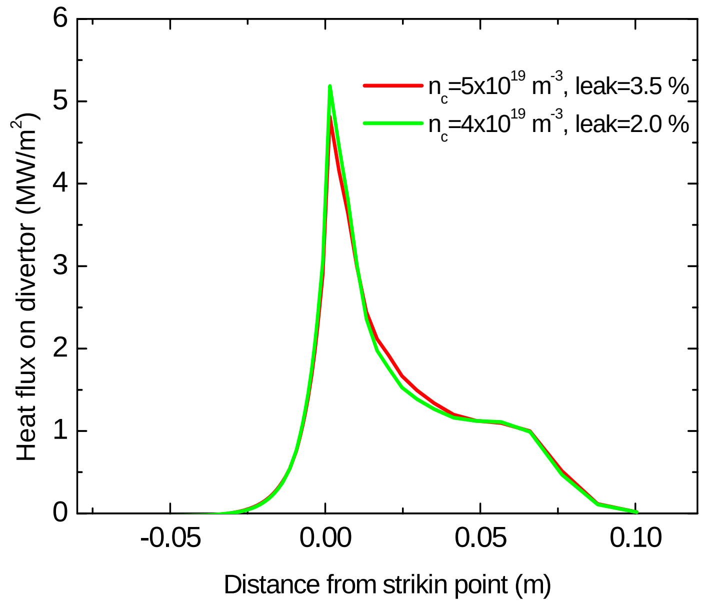

Results for various leakages at different powers

When midplane density is $1.5 \sim 2\times10^{19}\ \mathrm{m^{-3}}$, divertor heat flux is maximized.

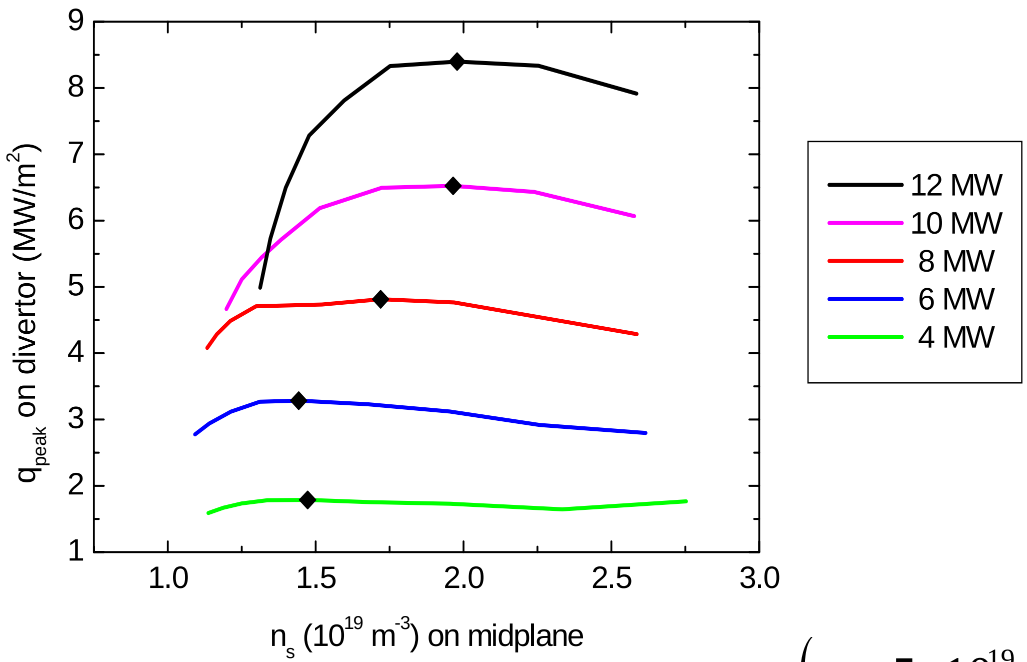

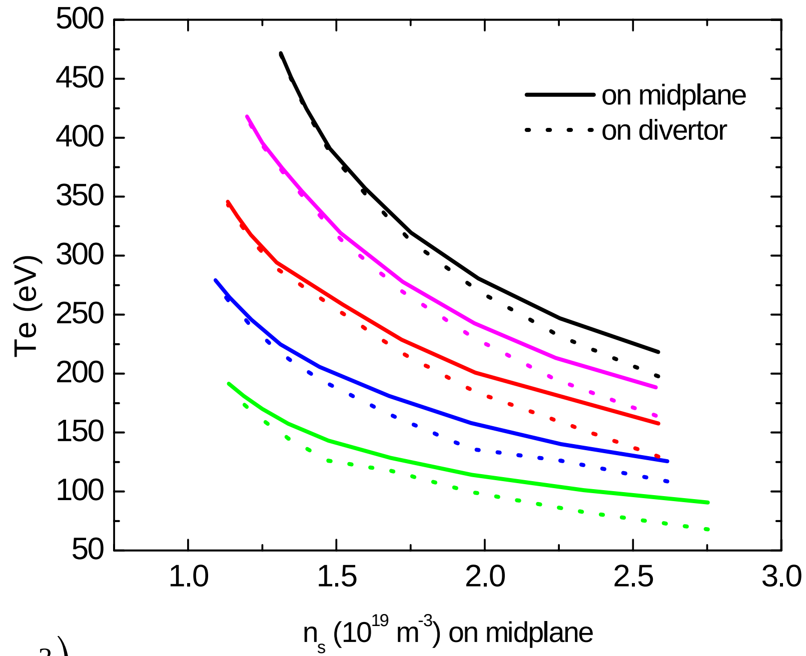

$$\left(n_c = 5\times10^{19}\ \mathrm{m^{-3}}\right)$$

Results for various powers $\left(n_c = 5\times10^{19}\ \mathrm{m}^{-3},\ \mathrm{leak}=3.5\%\right)$

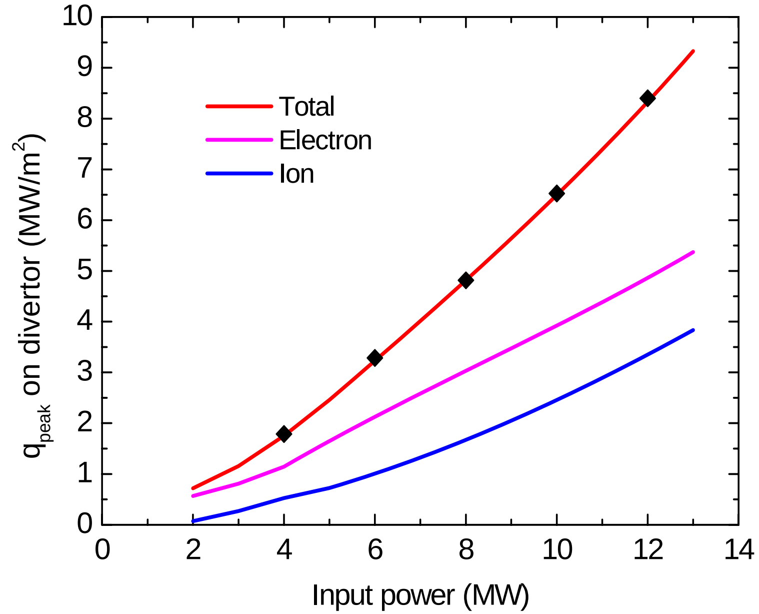

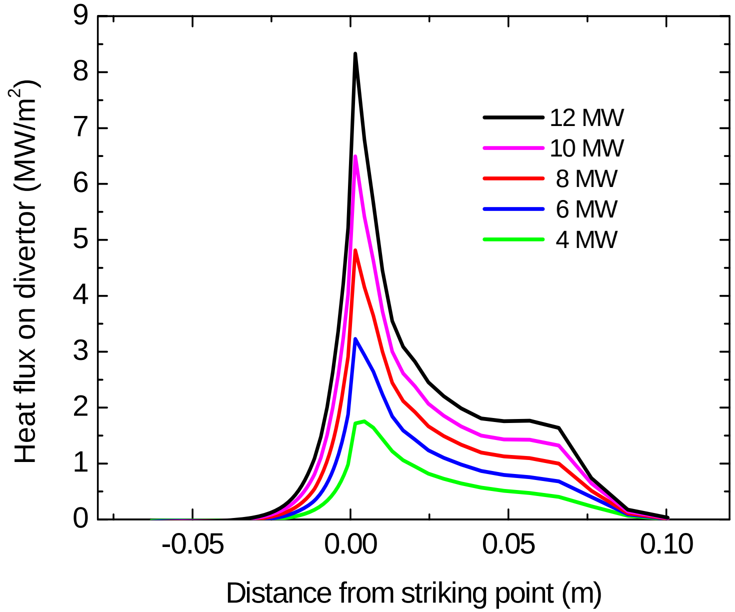

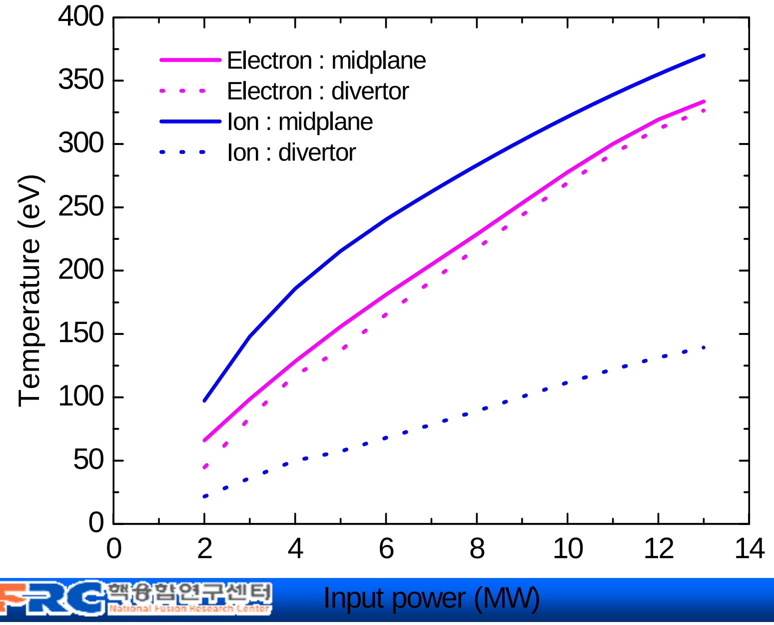

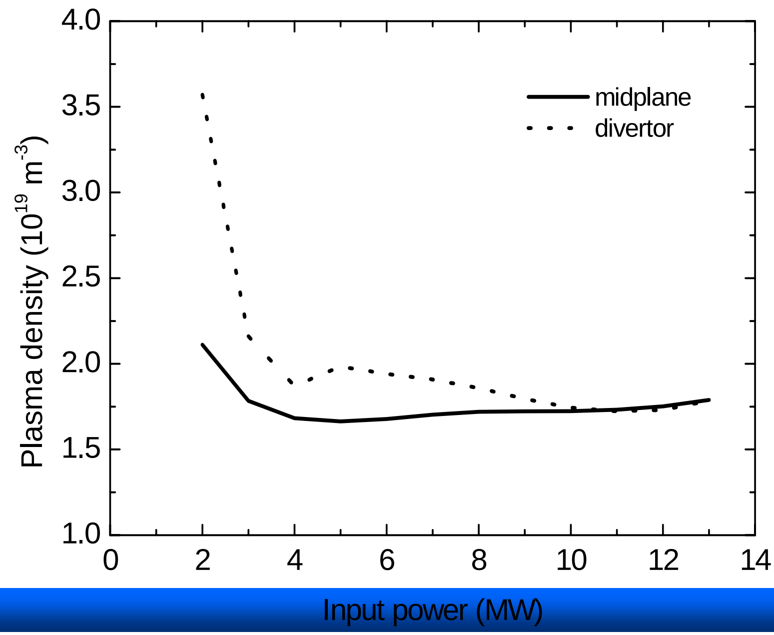

Divertor heat reduction by C impurity

$$\left(n_c = 5\times10^{19}\ \mathrm{m}^{-3},\ \mathrm{leak} = 3.5\,\%\right)$$

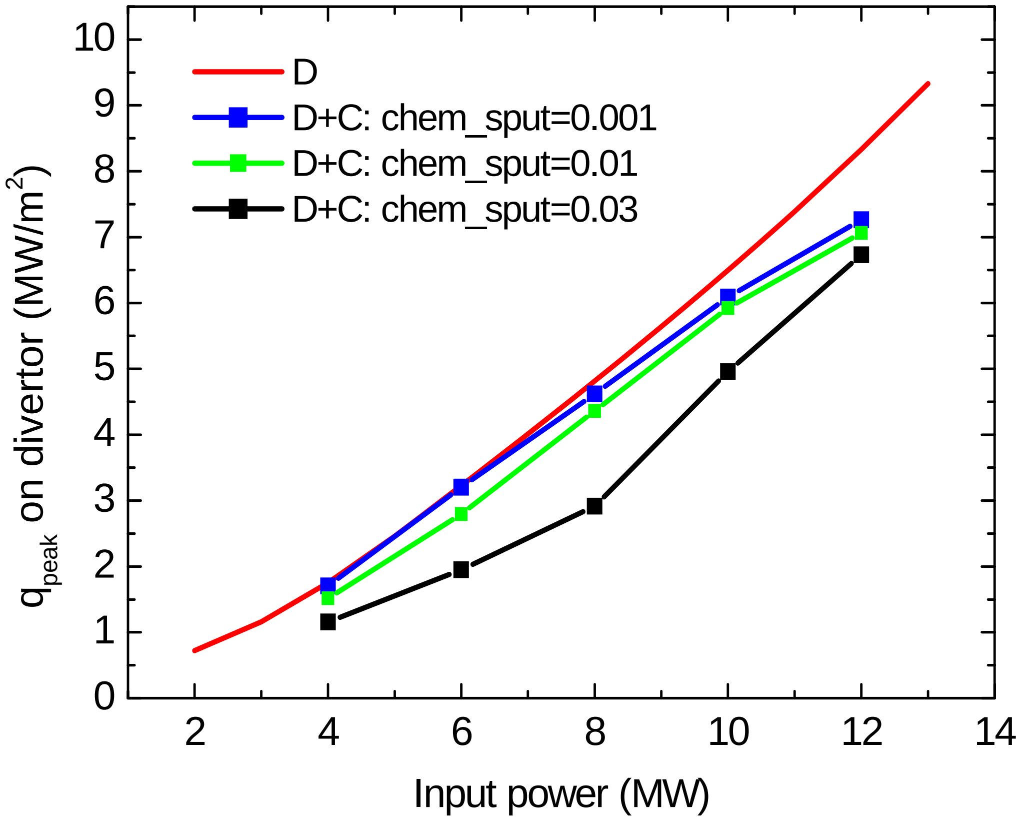

Carbon concentrations

4MW

$$\left(n_c = 5\times10^{19}\ \mathrm{m}^{-3},\ \mathrm{leak} = 3.5\%\right)$$

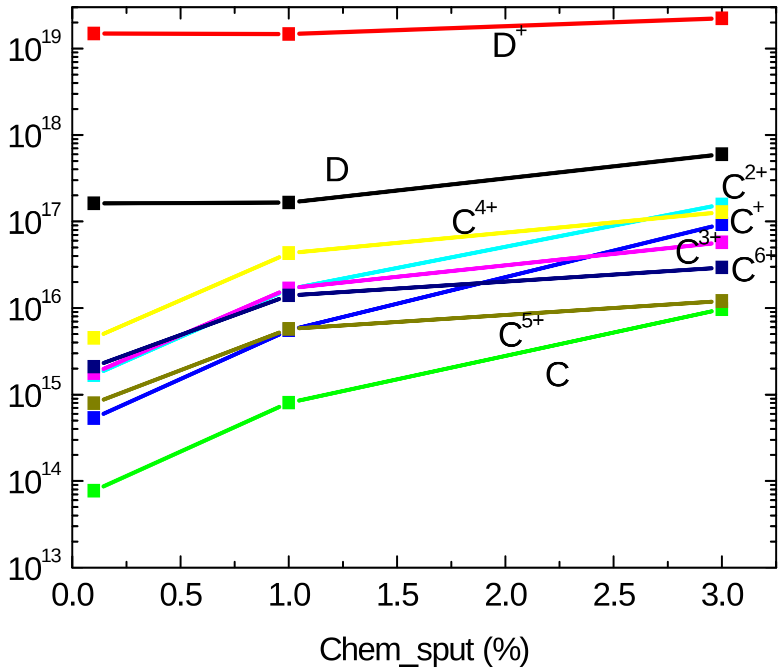

Divertor region

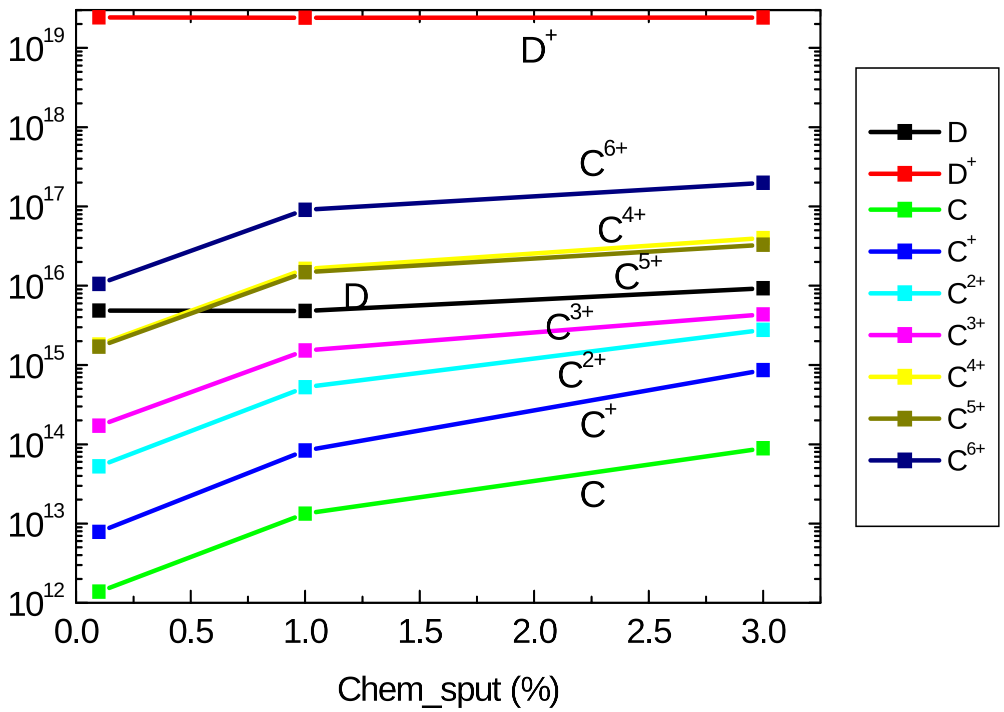

Core region

Simulation conditions (drift-on case)

Case I : No drift is considered.
Case II : Only diamagnetic drift is included.
Case III : All drifts are switched on.

Parameter	Value
Input power	4 MW
Plasma density at core boundary	3×10^{19} m^{-3}
Anomalous particle diffusivity D_{an}	2 m^2/sec
Anomalous thermal diffusivity χ_{an}	4 m^2/sec
Recycling coefficient at wall and divertor	1.0
Leakage factor in private region by pumping	0.3 %
Decay length at wall boundary	0.03 m

Effect of cross-field drifts on density distribution

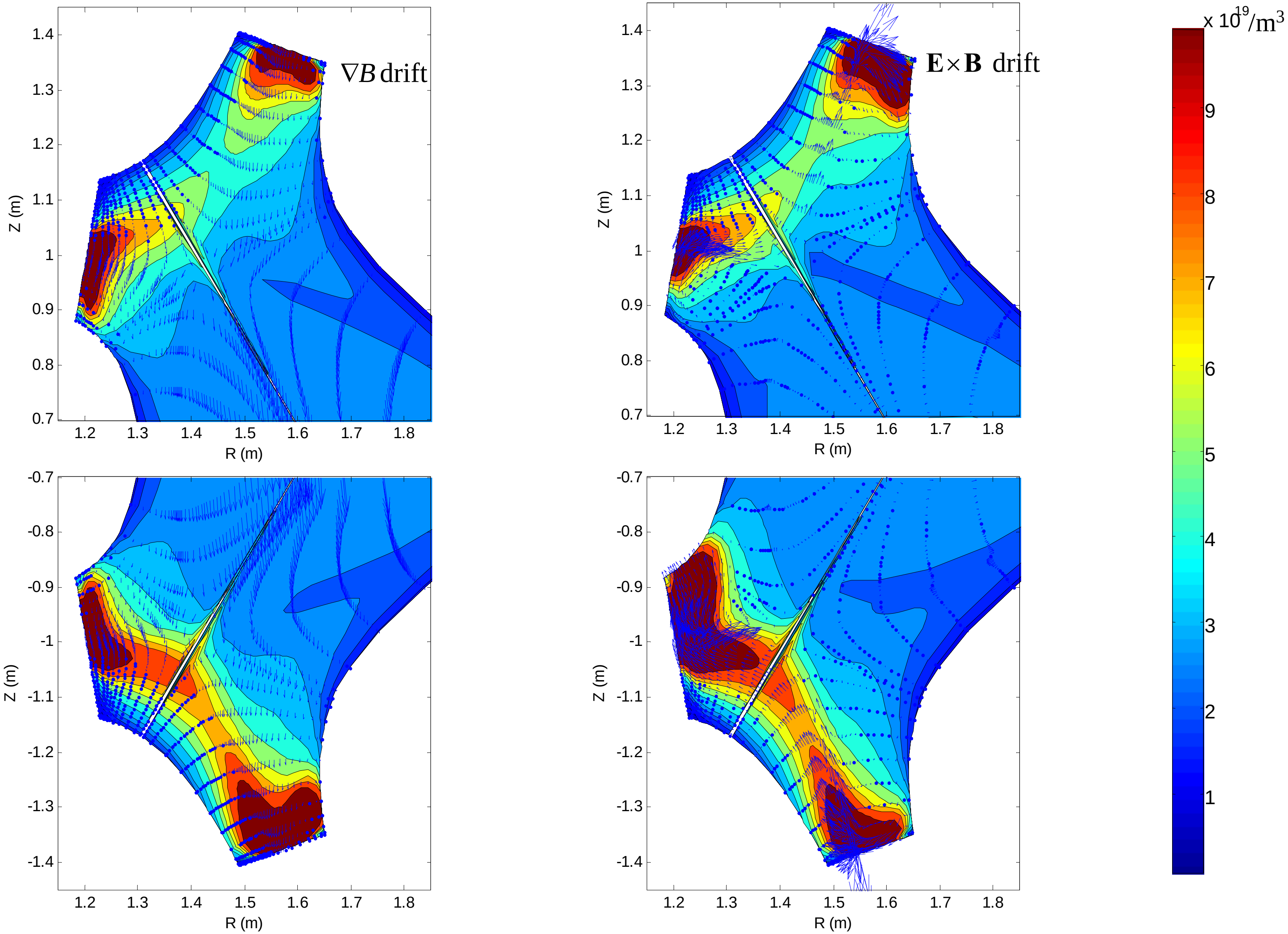

Case II   Case III

Heat load to divertors

$$\left(D_{an}=2\mathrm{m}^2/\mathrm{s},\ \chi_{an}=4\mathrm{m}^2/\mathrm{s}\right)$$

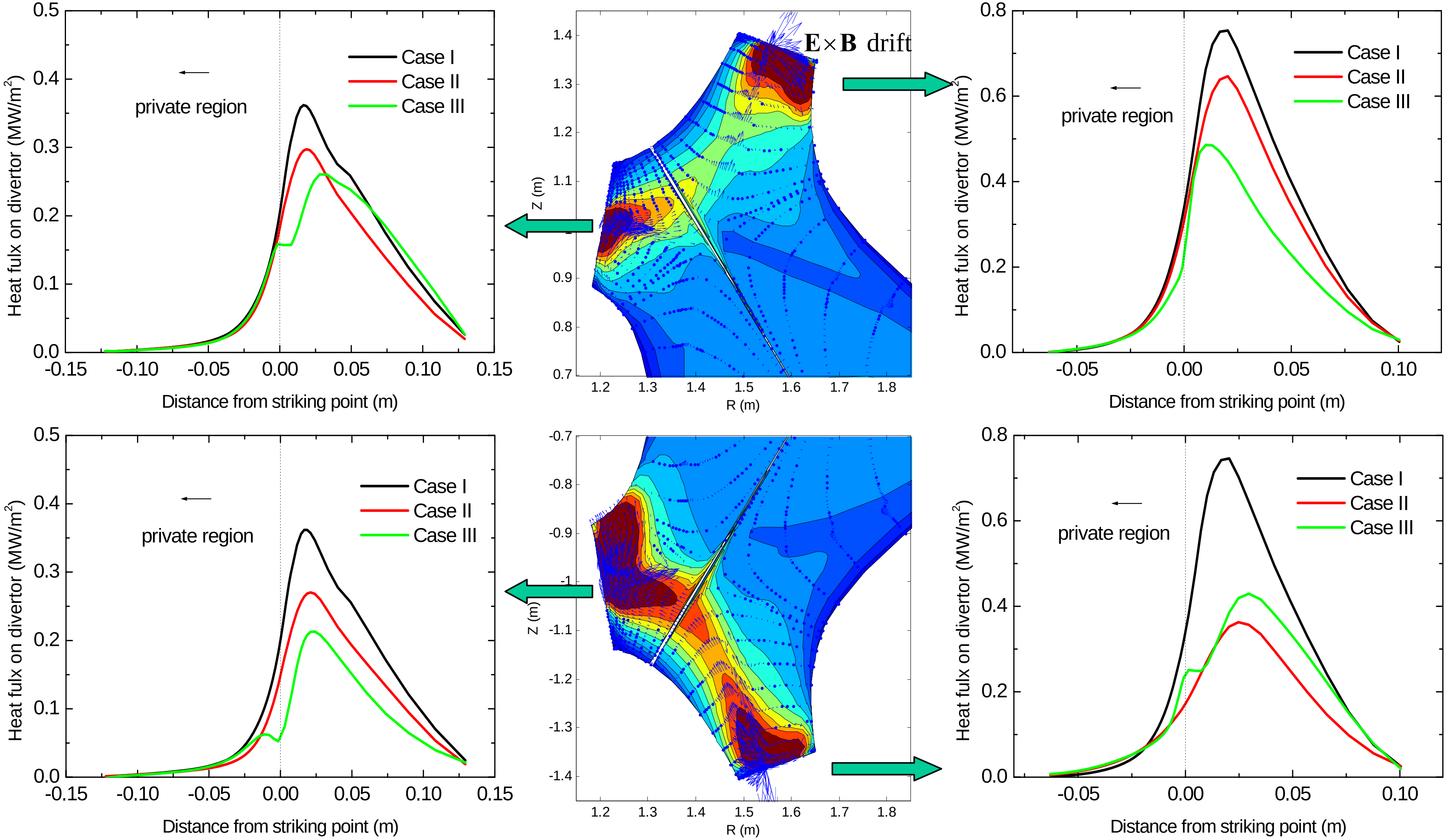

Heat load to divertors

$$\left(D_{an}=1\text{m}^2/\text{s}, \chi_{an}=2\text{m}^2/\text{s}\right)$$

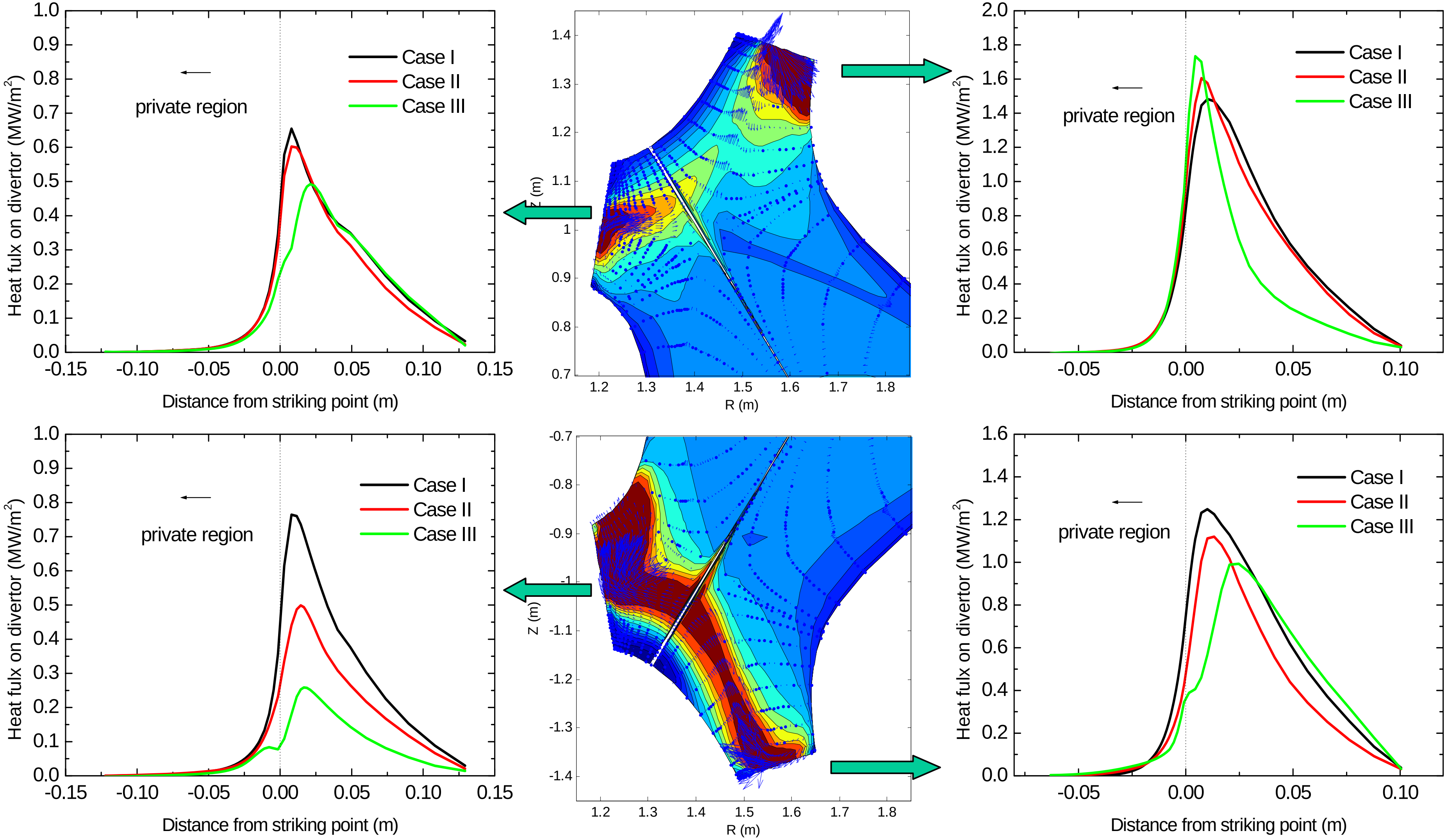

Total heat load to divertors and wall

		Total heat load (MW)		
		Case I	Case II	Case III
D_{an}=2m²/s χ_{an}=4m²/s	Divertor	1.30	0.97	0.89
	Wall	1.91	2.06	2.02
D_{an}=1m²/s χ_{an}=2m²/s	Divertor	2.38	1.82	1.52
	Wall	1.12	1.26	1.17

Concluding Remarks

- Assembly of KSTAR will be finished in Aug this year.

- 1st plasma is scheduled in the mid of next year.

  during this campagin, the various startup configuration for superconducting tokamak will be explored.

- For short-pulse operation, graphite will be suitable for heat removal both the limiter and divertor area.

- PWI modeling will be continued including density control and impurity migration.

We hope KSTAR will be soon one of the best machines for the PSI research…

We need your valuable experience definitely!

Thank you!